Chem Soc Rev

The biosafety of lanthanide upconversion nanomaterials

Journal:	*Chemical Society Reviews*
Manuscript ID:	CS-REV-05-2014-000175.R1
Article Type:	Review Article
Date Submitted by the Author:	28-Jul-2014
Complete List of Authors:	Li, Fuyou; Fudan University, Institute of Advanced Materials Sun, Yun; Fudan University, Department of Chemistry Feng, Wei; Fudan University, Chemistry Yang, Pengyuan; Fudan University, Department of Chemistry Huang, CHunhui; Fudan University, Department of Chemistry,

Chemical Society Review RSCPublishing

Review

The biosafety of lanthanide upconversion nanomaterials

Cite this: DOI: 10.1039/x0xx00000x

Yun Sun,[a] Wei Feng,[a] Pengyuan Yang,[a] Chunhui Huang,[a] and Fuyou Li*[a]

Received 00th January 2012,
Accepted 00th January 2012

DOI: 10.1039/x0xx00000x

www.rsc.org/

Lanthanide upconversion nanophosphors (UCNPs) show unique upconversion luminescence where lower-energy photons (such as near-infrared (NIR) excitation) are converted into higher-energy photons covering the NIR to the UV region, and are considered to have a bright future in clinical translation. As UCNPs are used in a significant number of potential bio-applications, their biosafety is important and has attracted significant attention. In this critical review, recent reports regarding the cellular internalization, biodistribution, excretion, cytotoxicity and *in vivo* toxic effects of UCNPs are reviewed. In particular, the studies which evaluated the association between the chemical and physical properties of UCNPs and their biodistribution, excretion, and toxic effects are presented in detail. Finally, we also discuss the challenges of ensuring the biosafety of UCNPs *in vivo*. (168 references).

1. Introduction

Upconversion luminescence (UCL) is a nonlinear, anti-Stokes process in which the absorption of two or more low-energy photons leads to the emission of one higher-energy photon.[1-4] Inorganic crystalline materials embedded with lanthanide ions (activators, such as Er^{3+} and Tm^{3+}) provide multiple intermediate metastable 4f excited states which can generate effective UCL emission.[1] In comparison to organic dyes and semiconductor quantum dots, lanthanide upconversion nanophosphors (UCNPs) show superior chemical and optical properties, including large anti-Stokes shifts, sharp emissions, long luminescence lifetimes, and high resistance to photobleaching.[1, 5-12] To date, UCNPs have been used in diverse research fields, such as solar cells,[13] three-color and solid-state display.[14]

In particular, due to the ultralow background, UCNPs as high-contrast luminescent probes can significantly improve the sensitivity and detection limits *in vitro* and *in vivo*.[15-23] Moreover, under continuous-wave near-infrared (NIR) excitation at 980 nm, Yb/Tm-codoped nanocrystals display UCL emission at 800 nm.[1] Using Yb/Tm-codoped UCNPs as a NIR-to-NIR emitting probe, the imaging depth *in vivo* has exceeded 2 cm,[22, 23] and the detection threshold of *in vivo* bioimaging was less than 1000 cells.[21] As a result, UCNPs have been used in biology and medical science in the fields of biodetection,[24-28] tumor imaging,[20, 29, 30] angiogenesis imaging,[31], lymph imaging,[22, 32-36] multimodality bioimaging,[31, 37-39] drug delivery[40, 41] and photodynamic therapy[42-45]. With their increasing bioapplication, the potential dissemination of UCNPs and their interactions in the human body have increased. Unfortunately, no systematic review concerning the biosafety of UCNPs has been reported. This review focuses on the distribution, excretion, and toxicity of UCNPs *in vitro* and *in vivo*, in relation to their stability, nanoparticle size, surface charge and dosage.

2. Internalization of UCNPs into cells

Cell internalization and the distribution sites of nanomaterials in cells determine the exposed cell organelle and thus the manner of induced toxic effects in cells and animals.[46] Therefore, the investigation of internalization and distribution sites of UCNPs in cells is important in biosafety assessment.

The plasma membrane is a selectively permeable membrane that defines the boundary and maintains the essential intracellular environment of the cell. Different from small molecules, nanomaterials are incapable of crossing the plasma membrane on their own and are generally internalized through endocytosis. These endocytosed nanomaterials are confined to endolysosomes and are incapable of reaching the cytosol.[47] Previous studies have shown that nanomaterials are often internalized into the cells *via* a process termed pinocytosis,[47, 48] which is a type of endocytosis that involves at least four basic mechanisms: macropinocytosis (>1 μm), clathrin-mediated

endocytosis (~120 nm), caveolae-mediated endocytosis (~60 nm), and clathrin- and caveolae-independent endocytosis.

Although there are many reports related to the internalization of UCNPs into cells, both tumor cells and normal cells, not all UCNPs can enter cells. The kinetics, amount, and mechanism of cellular uptake of UCNPs vary depending on a number of factors, such as size of nanoparticles, physicochemical properties of the surface ligand of the nanoparticles and incubation conditions. Herein, except mark with hydrodynamic diameter, the diameter of the nanoparticles stands for the data observed from transmission electron microscopy (TEM).

The most common interactions, electrostatic interactions, between the charged UCNPs and the negatively charged plasma membrane of cells, will largely affect the cytotoxicity and uptake efficiency of UCNPs. For example, Wong *et al.*[49] demonstrated that the surface charge of UCNPs largely determines their cellular uptake efficiency. Positively charged polyetherimide (PEI)-modified $NaYF_4$:Yb,Er nanoparticles (PEI-UCNPs, (50 nm, 51.1 mV) were clearly observed in cells following incubation. In contrast, after incubation of neutral polyvinylpyrrolidone (PVP) modified $NaYF_4$:Yb,Er nanoparticles (PVP-UCNPs, 50 nm, 10.2 mV) and negative polyacrylic acid (PAA) modified $NaYF_4$:Yb,Er nanoparticles (PAA-UCNPs, 50 nm, −22.6 mV) under the same incubation and image acquisition conditions, only a few illuminated spots with dim brightness in cells were observed. Further quantification data from inductively coupled plasma mass spectrometry (ICP-MS) indicated that after treatment with different UCNPs of 200 μM yttrium for 24 h, positive cellular uptake of PEI-UCNPs was 5 times that of neutral PVP-UCNPs (Figure 1). Negative PAA-UCNPs showed the lowest cellular uptake efficiency. These results indicated that the positive charge greatly enhanced cellular uptake of UCNPs, which was significantly higher than its neutral and negative counterparts.

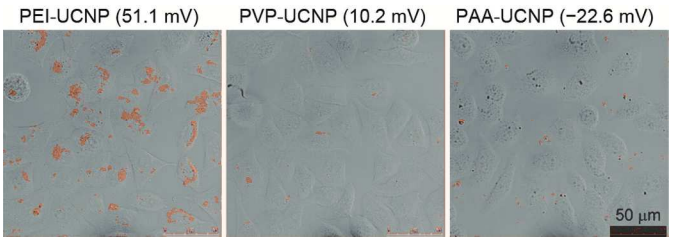

Figure 1. Confocal upconversion luminescent images of HeLa cells following 24 h incubation with $NaYF_4$:Yb,Er nanoparticles (50 nm, 50 μg mL^{-1}) with different charge, such as PEI-UCNP (51.1 mV), PVP-UCNP (10.2 mV), or PAA-UCNP (−22.6 mV). Scale bar = 50 μm. Reproduced with permission from ref. 49.

Several studies have also shown the uptake of negatively charged nanoparticles into cells. For example, our group found that citrate-modified $NaY_{0.2}Gd_{0.6}F_4$:$Yb_{0.18}$,$Er_{0.02}$ (~20 nm) with a charge of -18.1 mV were internalized by KB cells after 1 h incubation.[50] In addition, sodium glutamate and diethylene triamine pentacetate acid modified $NaLuF_4$:Yb,Er,Tm nanoparticles with a charge of -28.6 mV were also internalized by HeLa cells after 7 h incubation.[35] It should be noted that the absorption of serum protein *in vitro* or *in vivo* will significantly change the hydrodynamic size and surface property such as the charge.

Interestingly, increasing the incubation concentration of UCNPs significantly improved the rate of internalization.[49, 51-54] For example, Wong *et al*. demonstrated that $NaYF_4$:Yb,Er nanoparticles (50 nm) with PEI, polyvinylpyrrolidone (PVP) and polyacrylic acid (PAA) as surface ligands displayed significant different zeta-pential of 51.1, 10.2, and −22.6 mV, respectively. After 24 h incubation, these different UCNPs showed concentration-dependent cellular uptake in both HeLa and U87MG cell lines. The higher concentration induced a higher risk of toxicity. Therefore, the incubation concentration should be optimized according to needs.

In a typical study, Hyeon *et al.*[19] found that most of the amphiphilic PEG–phospholipids-coated $NaYF_4$:Yb,Er nanoparticles (30 nm) or their aggregates in cells display random spatial fluctuations with relatively low amplitudes, while some of the UCNPs undergo abrupt directed movements, indicating intracellular transport of vesicle-encapsulated nanoparticles in the endocytic pathway. The trajectory of UCNPs in cells is composed of multiple dynamic phases with a distinct transport speed, and UCNPs were actively transported by intracellular motor proteins on the microtubules or actin filaments, and microtubule-dependent motor proteins such as dyneins and kinesins are responsible for most active transport. In further studies,[55] the inward distribution shift of PEG-phospholipids coated $NaYF_4$:Yb,Er nanoparticles (UCNPs, 35 nm) was considered the consequence of particle transport operated by the microtubule-dependent motor proteins, dyneins being predominant over kinesins in this early stage.

Although many groups have reported that UCNPs can be taken up by living cells, a detailed investigation of the internalization process of UCNPs has rarely been carried out. Hyeon *et al.*[55] reported that the internalization of 35 nm Polyethylene glycol (PEG) modified $NaYF_4$:Yb,Er nanoparticles (PEG-UCNPs) into the cytoplasm was a result of endocytosis using an inhibition experiment. After adding cytochalasin D, which disrupts the actin filaments that play an important role in endocytosis, PEG-UCNPs remained around the plasma membrane without being internalized, indicating the endocytosis process of UCNPs. Wong *et al.*[49] constructed red fluorescent protein tagged clathrin (RFP-clathrin) and caveolae (RFP-caveolae) plasmids and independently expressed each plasmid into HeLa cells. After incubation with HeLa cells, polyetherimide (PEI) modified $NaYF_4$:Yb,Er nanoparticles (PEI-UCNPs, 50 nm, 51.1 mV) colocalized with RFP-clathrin at all time-points, but not RFP-caveolae. Clathrin vesicles were shown to move together with PEI-UCNPs from the cell surface to the rim of the nuclear envelope, suggesting that PEI-UCNPs entered HeLa cells mainly through clathrin-mediated endocytosis. Unfortunately, few investigations of the distribution site of UCNPs in cells have been reported. The potential distribution sites of UCNPs include the membrane,

lysosomes, and cytoplasm, but not the nucleus, endoplasmic reticulum, or mitochondria.

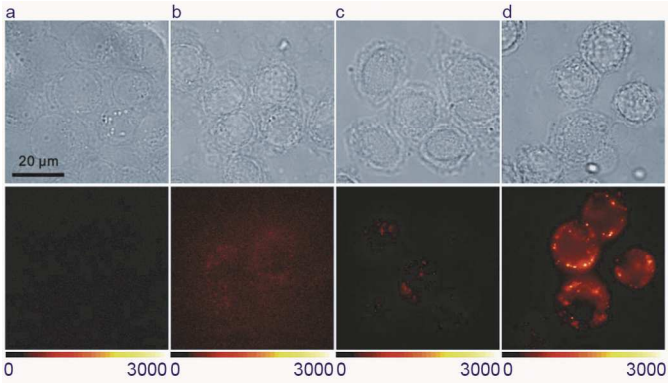

Figure 2. Cellular uptake of 20 nm UCNPs in SK-BR-3 cells. (Top row) Bright field images. (Bottom row) Luminescence images with the excitation at 980 nm and the detection at 400–700 nm. Cells were incubated with the UCNPs ($NaGdF_4$:Yb,Er, 20 nm) with 100 mg mL^{-1} of Gd^{3+} concentration at 37 °C. (a) Cells incubated without UCNPs. Incubation time was (b) 30 min, (c) 2 h, (d) 4 h. Reproduced with permission from ref. 39.

The internalization of UCNPs is reported to be slow. Hyeon *et al.* reported that following the incubation of SK-BR-3 cells with 20 nm $NaGdF_4$:Yb,Er nanoparticles (UCNPs) for 2 h caused little internalization into cells, and an obvious UCL signal appeared 4 h after incubation (Figure 2).[39] After 24 h incubation, internalization of 1.3×10^4 particles in each cell was measured by inductively coupled plasma atomic emission spectroscopy (ICP-AES).[39] These authors also investigated the internalization process of hexagonal 50 nm PEG-modified $NaYF_4$:Yb,Er nanoparticles (PEG-UCNPs) by HeLa cells by integrating the luminescence intensity in cells. When the incubation time was ~ 5 h, the internalization of PEG-UCNPs peaked at 6 h after incubation, and the internalized PEG-UCNPs then underwent exocytosis.[55]

3. Distribution of UCNP in *Caenorhabditis elegans* and zebrafish

Caenorhabditis elegans (*C. elegans*) is one of the simplest multicellular eukaryotic organisms with complete organs such as intestine, muscle, hypodermis, gonad and nervous system. The zebrafish is a tropical freshwater fish that has been used as an important vertebrate model organism in scientific research.[56] The advantage of *C. elegans* and zebrafish as model animals in optical imaging is their transparent body, which allows excellent light penetration.

Yan *et al.*[18] reported that after feeding with a mixture of B-growth media and PEI-modified $NaYF_4$:Yb,Tm nanoparticles (PEI-UCNPs, 42 nm) for 2 h, 6 h, and even for 12 h, most of the PEI-UCNPs were found in the gut of *C. elegans* hermaphrodites (Figure 3). Interestingly, the PEI-UCNPs existed only in the gut, not in the cells, indicating that the PEI-UCNPs could not penetrate the membrane of intestinal cells and be absorbed into the body. Moreover, no significant difference in the ingestion of PEI-UCNPs was observed between the hermaphrodite and the male. Similar results have been reported by other groups.[56-58]

With regard to zebrafish, Cai *et al.*[59] injected 2 μL LaF_3:Yb,Er@SiO_2 (core: 7~10 nm, silica shell: 3 nm) solution (UCNPs@SiO_2, 1 mg mL^{-1}) into the pectoral fin vertically, and a high accumulation of UCNPs@SiO_2 in the intestine was observed 24 h after injection. In addition, no significant amount of UCNPs@SiO_2 was measured in the cells of zebrafish.

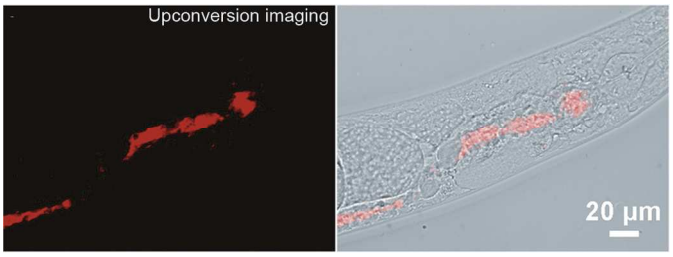

Figure 3. False-colored NIR upconversion luminescent imaging of *C. elegans* fed with the mixture of B-growth media and $NaYF_4$:Yb,Tm nanoparticles for 6 h. Reproduced with permission from ref. 18.

4. Distribution of UCNP *in vivo*

The administration type of UCNPs into living mouse is relative to its biodistribution within the body of the animal. Currently, most of the reported UCNPs were focused on the intravenous injection.

4.1 Distribution of intravenously injected UCNP in mouse

Table 1 summarizes the *in vivo* biodistribution site of intravenously injected UCNPs. It can be deduced from Table 1 that, except for some ultrasmall nanoparticles, the final deposition site was mainly the liver and spleen, regardless of size and surface ligand of the UCNPs. This is ascribed to capture by the mononuclear phagocyte system (MPS) which is a part of the immune system and consists of phagocytic cells located in reticular connective tissue. However, the ratio of dosage in these organs was different and depended on the size, shape, surface ligand, and time after injection of UCNPs.

Surface property is one of the determinants of UCNP accumulation *in vivo*. For example, PEG was the most effective surface ligand to affect the pharmacokinetics of nanoparticles *in vivo*. The US Food and Drug administration (FDA) approved a linear polyether diol PEG that exhibited a low degree of immunogenicity and antigenicity, by which nanoparticles could obtain a longer circulation time in blood.[60] The highly flexible polymer chains of PEG tend to generate a "conformational cloud" around the nanoparticles, which have a large total number of possible conformations. The "conformational cloud" prevents interactions with blood components as well as protein interactions such as enzymatic degradation or opsonisation followed by uptake by the MPS.[61] The higher the rate of transition from one conformation to another, the more the

polymer exists statistically as a "conformational cloud". To date, PEG has been used to extend the circulation time of UCNPs.[46, 50, 53, 54, 62-65] Using gamma counter analysis, our group investigated the blood retention time of PEG-modified $NaYF_4$:Yb,Er,^{153}Sm nanoparticles (PEG-UCNPs(^{153}Sm), 5±2.2 nm) injected into mice *via* the tail vein.[65] The radioactive value of blood was 16.5±0.6%ID/g at 5 min post-injection, then gradually decreased to 10.34±0.70%ID/g at 0.5 h and 6.84±1.0%ID/g at 1 h post-injection. The blood circulation of PEG-UCNPs(^{153}Sm) followed a typical two-compartment biexponential model. After a rapid decay with a first phase half-life of 0.4±0.1 h for biodistribution, these PEG-UCNPs(^{153}Sm) in circulating blood exhibited a long second phase half-life of 4.3±0.6 h for elimination.

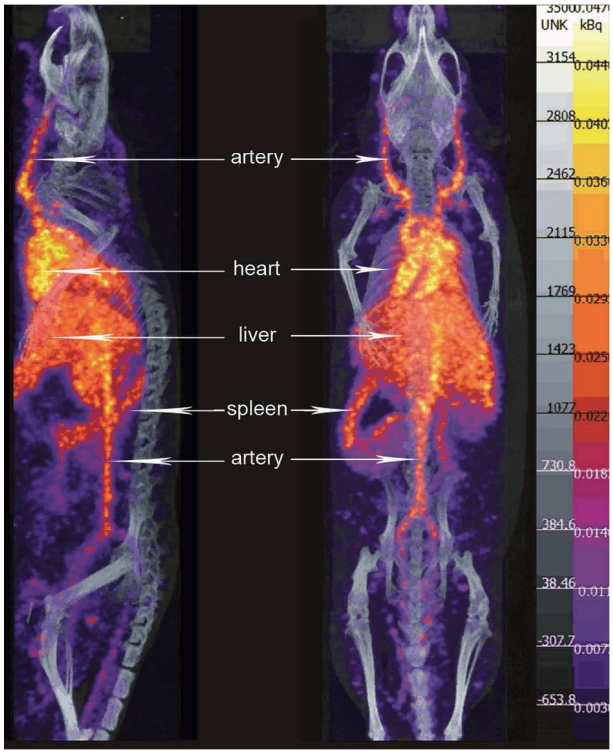

Figure 4. SPECT/CT imaging *in vivo* of mouse after intravenous injection of EDTMP modified UCNP ($NaLuF_4$:Yb,Tm,^{153}Sm, 37.8 nm) at 1 h. All images were acquired under the same instrumental conditions. Reproduced with permission from ref. 66.

Moreover, we found that ethylene diamine tetramethylenephosphonic acid (EDTMP) as the surface ligand could not only significantly improve the dispersity of $NaLuF_4$:Yb,Tm nanoparticles (EDTMP-UCNPs), but also extended the circulation time of UCNPs in blood and may thus be used for blood pool imaging.[66] Figure 4 shows a single photon emission computed tomography (SPECT) image of ^{153}Sm-labeled EDTMP-UCNPs (37.8 nm) in the circulation after intravenous injection in a Kunming mouse. An intense signal was detected in the blood during the first 30 min. The heart, carotid artery, vertebral arteries, and superior epigastric artery of the mouse were clearly displayed. The extension of circulation time was mainly ascribed to the adherence of EDTMP-UCNPs onto red blood cells.

SiO_2 is another important factor in changing the surface property of UCNPs. For example, Zhang *et al.*[67] investigated the *in vivo* biodistribution of silica-coated $NaYF_4$:Yb,Er nanoparticles (UCNP@SiO_2) with 21±0.5 nm in core's diameter and the shell thickness of approximately 8±1.5 nm. After intravenous injection of UCNP@SiO_2, yttrium determination showed the highest proportion in the lung at 29.2 and 18.6 mg/L/g, at 10 and 30 min post-injection, respectively. The second highest proportion was found in the heart at 18.0 and 10.9 mg/L/g, at 10 and 30 min post-injection, respectively. Both concentrations of UCNP@SiO_2 in the lung and heart decreased significantly to 0.45 and 0.04 mg/L/g, respectively, at 24 h post-injection. The concentration of UCNP@SiO_2 in the kidney remained the same at 7.7 mg/L/g at 24 h post-injection. In the spleen, the highest nanocrystal concentration at 30 min post-injection was 6.3 mg/L/g, while in the blood and liver, the concentration remained low throughout.

The targeting moiety can change the *in vivo* biodistribution sites and ratio of intravenously injected UCNPs, especially the ratio of accumulation in targeted tissue such as tumor. Our group reported the first example of targeted UCL imaging *in vivo* in living mouse using folic acid-modified UCNPs as a probe, on the basis of the high affinity of folic acid and its receptor.[30] To date, there is a series of targeting moieties used to decrease non-specific distribution, such as tripeptide Arg-Gly-Asp (RGD),[20] chlorotoxin,[68] heparin, basic fibroblast growth factor,[69] anti-Her2 antibody,[70] anti-claudin-4,[71] anti-mesothelin,[71] and rabbit CEA8 antibody.[70, 72]

The biodistribution of UCNPs in organs is not static. The ratio of UCNPs in organs changes at different times after injection. In our previous study,[73] 148 MBq ^{153}Sm-labeled and citrate-modified UCNPs ($NaLuF_4$:Yb,Tm,^{153}Sm, 22.1±2.2 nm) were injected into mice *via* the tail vein and quantification by SPECT imaging was used to track the dynamic change in biodistribution *in vivo* (Figure 5). 60 min after injection, ^{153}Sm signals were detected in the liver and spleen. The signal from the liver reached a peak at 238 min, and maintained the maximum value for 508 min. The signal intensity in the spleen increased quickly beyond 238 min and reached a peak at 508 min. After 508 min, the signals from the liver and spleen decreased.

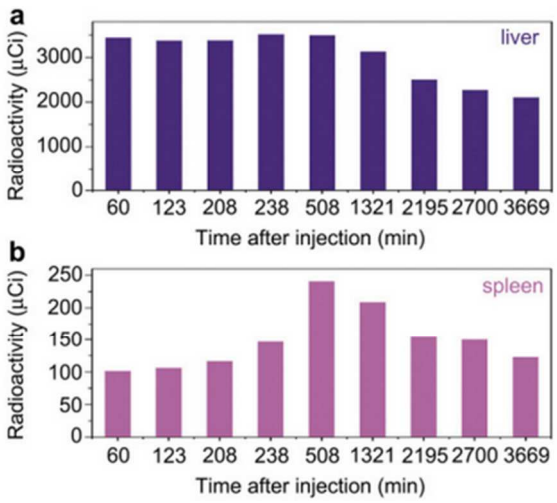

Figure 5. Quantification of citrate-modified UCNPs ($NaLuF_4$:Yb,Tm,^{153}Sm, 22.1±2.2 nm) located in liver (a) and spleen (b). Reproduced with permission from ref. 73

4.2 Distribution of intra-arterially injected UCNP in mouse

As an alternative pathway for the administration of drugs, intra-arterial (i.a.) infusion has been investigated for a long time and has been applied in clinical medicine. However, only one case of intra-arterial injection of UCNP was reported by our group. After intra-arterially injected PEG-modified nanocomposite $NaYF_4$:Yb,Tm@SiO_2 (core: ~20 nm; shell: ~8 nm) into the mouse, the nanocomposite PEG-UCNP@SiO_2 also mainly deposit in the liver and spleen.[74] Interestingly, for MCF-7 tumor-bearing mouse, the uptake of PEG-UCNP@SiO_2 by the tumors following intra-arterial (i.a.) injection was nearly three-fold higher than that obtained with intravenous (i.v.) injection. Although intra-arterial injection is not a novel technique in clinical test, the application of this technique for infusions of UCNPs will give a possible chance in the enhancement of tumor therapeutics.

4.3 Distribution of subcutaneously injected UCNP in mouse

The behavior of subcutaneously injected UCNPs is very different from that injected intravenously, as the nanoparticles can enter the lymph system. For example, 50 μL of citrate modified-$NaLuF_4$:Yb,Tm nanoparticles (cit-UCNPs, 17 nm, 2 mg mL^{-1}) was injected intradermally into the right hind limb of mice. 30 min after injection, lymph vessel images were recorded by X-ray microCT (Figure 6a), and clearly depicted lymphatic drainage. This demonstrated that the injected cit-UCNPs rapidly entered the lymphatic drainage within a few minutes and then entered the lymphatic vessels around the injection site, which was confirmed by UCL imaging (Figure 6b). Due to the relatively large size of cit-UCNPs, the nanoparticles had small diffusion coefficients and did not diffuse into normal tissue. Moreover, compared to small molecular agents, the flow velocity in lymph vessels was slow. Furthermore, UCL imaging in the same study revealed that the intradermally or subcutaneously injected cit-UCNPs did not tend to distribute into the main organs of the mouse in hours after injection. Similar results were observed in our previous work and other studies.[32]

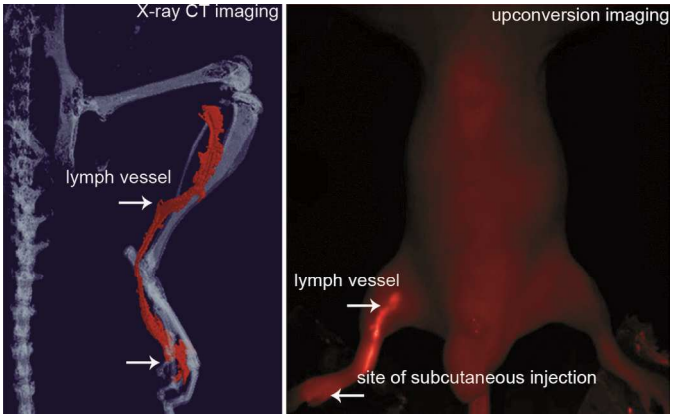

Figure 6. The behaviour of subcutaneously injected cit-UCNPs (17 nm, 2 mg mL^{-1}) 30 min after injection. Reproduced with permission from 36.

5. Excretion

Historically, the FDA requires that agents injected into the human body, especially diagnostic agents, should be completely cleared in a reasonable amount of time.[75] This policy makes sense in that total body clearance minimizes the area under the exposure curve. It is known that most drugs are mainly excreted through the hepatobiliary or renal route. Herein, we will introduce related studies on drug excretion of UCNPs by these two routes.

5.1 Hepatobiliary excretion

Hepatocytes, but not macrophages (Kupffer cells) serve as an important site for the elimination of foreign substances and nanoparticles through phagocytosis. Thus, all nanoparticles excreted *via* the biliary system are first catabolized through hepatocytes. However, the Kupffer cells meet intravenously injected nanoparticles before hepatocytes (Figure 7) and show higher phagocytic capacity than hepatocytes. Moreover, similar to all phagocytic cells in the MPS, nanoparticles unbroken by intracellular processes will remain within the cell and therefore will be retained by the body for a long time.[76]

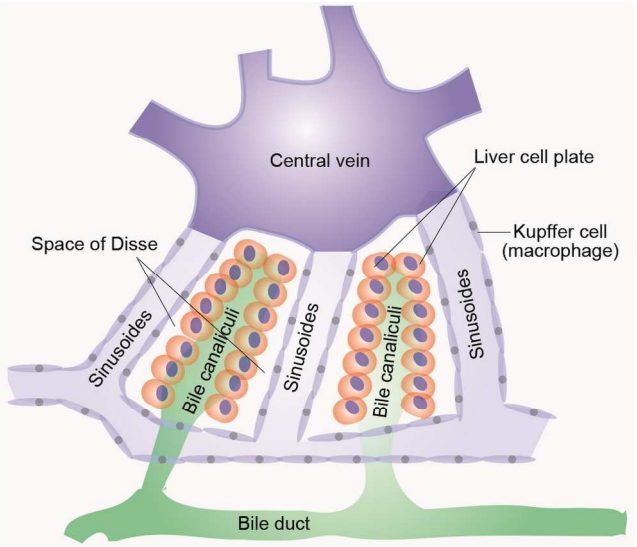

Figure 7. At the cellular level, hepatocytes are organized in cords and bathed by sinusoidal blood from the basolateral side; the canalicular membranes form the bile canaliculi. Bile flows in the opposite direction to blood and drains into bile ducts.[77] Reproduced with permission from 77.

The biliary excretion of UCNPs was monitored by our group using UCL imaging.[78] For *in vivo* biodistribution imaging studies, athymic nude mice were injected with 15 mg/kg of PAA-coated $NaYF_4$:Yb,Tm nanophosphors (PAA-UCNPs, 11.5 nm) *via* the tail vein. At 7 days post-injection, the presence of UCL signals in the intestinal tract indicated a clearance of PAA-UCNPs *via* hepatobiliary transport. At 21 days post-injection, the UCL signal was only detected in the intestinal tract and remained unchanged up to 90 days. At 115 days post-injection, almost no UCL signal was observed in the mice, showing that most of the PAA-UCNPs were excreted from the body of mice. We quantificatively investigated the biliary excretion of ^{153}Sm-radiolabeled and citrate-modified $NaLuF_4$:Yb,Tm nanoparticles (cit-UCNPs:^{153}Sm, ~60 nm of hydrodynamic size) using gamma counter detection.[73] A signal corresponding to only ~6% ID/g of cit-UCNPs:^{153}Sm was detected in total urine 300 min after intravenous injection, indicating that there was low renal excretion of ~60 nm cit-UCNPs:^{153}Sm. The autoradiography image indicated an obvious signal from cit-UCNPs:^{153}Sm in the intestine, indicating biliary excretion. However, this signal was weak, indicating that the excretion rate was slow. Similar results for biliary excretion was reported for PEG-modified $NaYbF_4$:Tm nanoparticles (hydrodynamic diameter of 56.9 nm), by ICP-MS measurement.[79]

Interestingly, compared to the nanoparticles before injection, the excreted UCNPs through the biliary route showed no significant changes. At the 3rd and 14th day post-injection of PEG-modified $NaGdF_4$:Yb,Er nanoparticles (PEG-UCNPs, 18.5±1.3 nm) in mice, Gao *et al.*[29] found that PEG-UCNPs in the feces showed no difference in size, size distribution, and shape, using TEM image analysis. This suggested that PEG-UCNPs within living mice were not transformed.

5.2 Renal excretion

Renal excretion is a desirable pathway for nanoparticle clearance, as the nanoparticles are not taken up by cells and involved in intracellular catabolism. Thus, the possibility of retention and cytotoxicity is significantly reduced. It is generally accepted that nanoparticle size is one of the critical determinants of excretion route.[76] During renal excretion, the smallest nanostructural dimensions are approximately 43 nm in diameter in the glomerular capillary wall.[80] However, considering the combined effects of several layers of glomerular capillary, the functional or physiologic pore size decreases to 4.5–5 nm in diameter.[81]

Recently, using gamma counter detection, we found that intravenously injected PEG-modified, ^{153}Sm-labelled $NaYF_4$:Yb,Er nanoparticles (PEG-UCNPs:^{153}Sm) with <10 nm of hydrodynamic diameter were observed in the bladder at a concentration of 5.28 ± 0.2%ID/g from 0.5 h to 6 h after injection.[65] The UCNPs:^{153}Sm were also found in the intestine at a concentration of 0.21±0.04%ID/g 1 h after injection. The result indicates that the size of UCNPs could affect the excretion of UCNPs. Moreover, these small PEG-UCNPs can be eliminated by two routes at the same time.

However, the particle size was not the only determinant of renal excretion. For example, 3.3 nm (hydrodynamic diameter) SiO_2 coated Gd_2O_3 nanoparticles were not excreted from the body, but were deposited in the liver and lung.[82] However, after modification with PEG,[82] the nanoparticles were found in the bladder 1 h after intravenous injection, indicating fast elimination by renal excretion.

5.3 Excretion time

The excretion time determines the exposure period of UCNPs in organs and tissues, and the degree of toxicity. Several studies on the excretion time of UCNPs have been reported.

Generally, small particles excreted by the renal route show fast excretion from hours to days, while large particles excreted by the biliary route takes longer from weeks to month and even years. Our group[78] reported that the complete excretion time of PAA-coated $NaYF_4$:Yb,Er nanoparticles (11.5 nm) was 115 days (Figure 8). In the studies by Liu and colleagues,[83] the PAA or PEG coated larger $NaYF_4$:Yb,Er nanoparticles (~30 nm) remained inside the mouse 90 days after injection, with only partial excretion. The half-life time of UCNPs excretion *in vivo* was also related to particle size. In addition, Gao *et al.*[29] prepared two PEG-modified UCNPs of different sizes, i.e., 18.5±1.3 nm ($NaGdF_4$:Yb,Er) and 5.1 ± 0.4 nm ($NaGdF_4$). The smaller nanoparticles exhibited an elimination half-life of 1.4 days, while for the larger nanoparticles this value was 7.0 days.

During the hepatobiliary excretion process, the clearance of UCNPs from the lung is usually quicker than from the liver and spleen. For example, using SPECT imaging and gamma counter detection, our group[73] demonstrated that at 3669 min after intravenous injection, the signals of citrate-modified UCNPs ($NaLuF_4$:Yb,Tm, 22.1 ± 2.2 nm) from the liver and spleen showed losses of 34% and 49%, respectively. The elimination

of UCNPs:^{153}Sm from the MPS seemed to be ongoing 120 h after injection. In particular, clearance from the lung (82.2%) was apparently quicker than that from the liver (69.9%) or the spleen (40%). Fortin *et al.*[84] have showed the excretion process of citrate coated NaY(Gd)F_4:Yb,Tm nanoparticles (23.0±1.7 nm) in 8 days. There was a 33% loss in the liver and a 43% increase in the spleen, which also indicated slow elimination in the liver and spleen. Similarly, the excretion of UCNPs in the lung was quicker than that from the liver and spleen, which showed a 57% loss. Gao *et al.*[29] reported that 87% elimination of $NaGdF_4$:Yb,Er nanoparticles (18.5±1.3 nm) took 30 days according to the results of ICP-AES.

However, due to the complicated process of UCNPs excretion, the excretion time of UCNPs will be dependent on many factors, including size and charge of UNCPs and surface ligand. To date, the fastest complete excretion time of UCNPs (PEI-modified, SiO_2-coated $NaYF_4$:Yb,Er nanoparticles, 50 nm in diameter) was 7 days, reported by Zhang *et al.*[67, 85] in addition, Shi *et al.*[79] reported that UCNPs were completely excreted 30 days after intravenous injection.

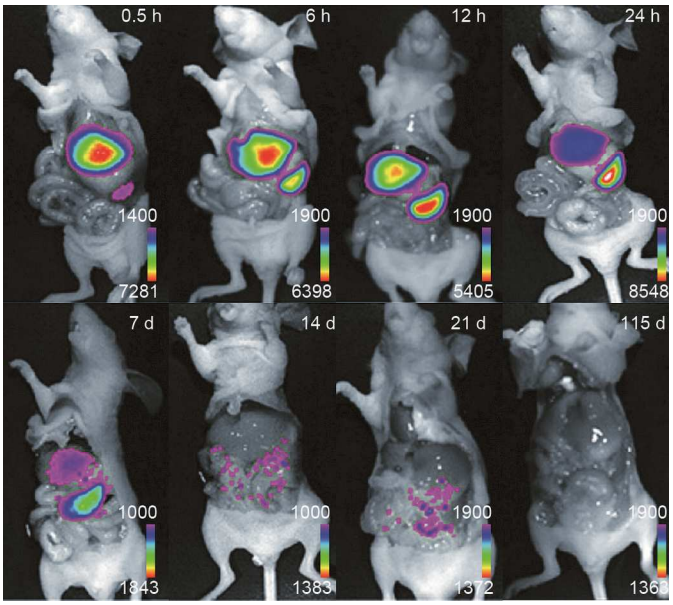

Figure 8. Upconversion luminescence imaging of athymic nude mice with intravenous injection of PAA-UCNPs ($NaYF_4$:Yb,Tm, 11,5 nm, 15 mg/kg) at different time points. Reproduced with permission from ref. 78.

6. Toxic effects of UCNP on cells

6.1 Toxic effects of UCNPs on cell viability

Many studies have been carried out to investigate the potential toxicity of UCNPs in cells. Mitochondrial metabolic activity has generally been used to investigate the influence of UCNPs on cell viability of normal or tumor cells. The usual methods include MTT (methyl thiazolyl tetrazolium), MTS ((3-(4,5-dimethylthiazol-2-yl)-5-(3-carboxymethoxyphenyl)-2-(4-sulfophenyl)-2*H*-tetrazolium, sodium salts), and CCK-8 assays. To date, various concentrations of UCNPs in the range of 0.05~20000 μg mL^{-1} and with different incubation periods ranging from 1 to 336 h have been studied. Table 2 gives the selective data of cell viability after incubation with UCNPs of different sizes (5~400 nm) and surface charge for no less than 24 hours. More than 75% of cells were viable in most cases, demonstrating the weak toxic effects of UCNPs on cell viability in these conditions. For example, in 2008, we[86] investigated the cytotoxicity of mPEG-LaF_3:Yb,Ho (15 nm) on KB cells at different concentration and found that about 80% of incubated cells was viable even at a high incubation concentration of 500 μg mL^{-1} and an incubation time of 12 hours.

Noticely, the viability of cells treated with UCNPs mainly depended on the incubation time and concentration.[17, 19, 20, 30, 32, 33, 39, 41, 50, 62, 67, 68, 71, 78, 85-101] A type example was reported by Zhang *et al.*[67] As shown in Figure 9, the cell viability of two skeletal myoblasts and marrow-derived stem cells (BMSC) decreased when the incubation concentration of the $NaYF_4$:Yb,Er@SiO_2 (~30 nm) nanocomposite increased from 1 to 100 μg mL^{-1}. At a high incubation concentration of 100 μg mL^{-1}, approximately 63% of these cell were viable.

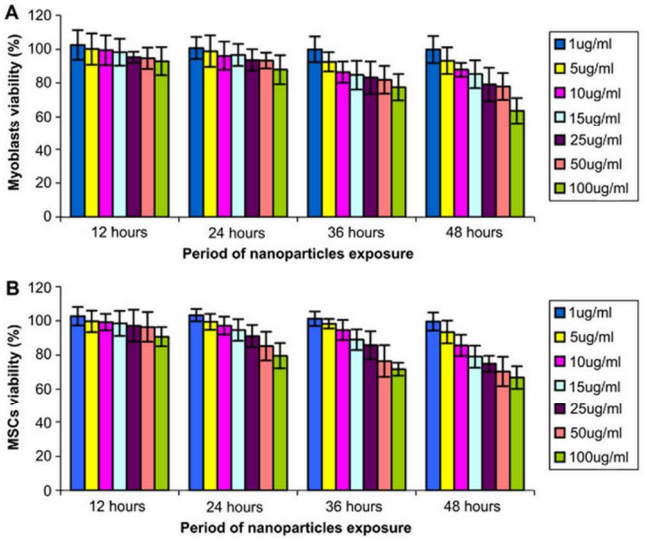

Figure 9. Cell viability of (a) skeletal myoblasts and (b) BMSCs after 12 h, 24 h, 36 h and 48 h exposure to 1, 5 , 10, 15, 25, 50 and 100 μg mL^{-1} of $NaYF_4$:Yb,Er@SiO_2 nanocomposites (~30 nm). Reproduced with permission from ref. [67].

6.2 Toxic effects of UCNP on cell behaviour

UCNPs have been used successfully as photoluminescent probes to track the behavior of normal cells and tumor cells, and low toxic effects on cell behaviour have been observed. Zhang *et al.*[52] used SiO_2-coated $NaYF_4$:Yb,Er nanoparticles (UCNP@SiO_2, 50 nm) as a luminescent probe to dynamically track live myoblast cells *in vitro* and in a living mouse model of a cryoinjured hind limb using confocal microscopy. The UCL signal of UCNP@SiO_2 tracking transplanted cells in mouse limb muscle was followed over 4 h (Figure 10), and revealed subtle migratory activity of the transplanted cells. Liu *et al.*[102]

labeled mesenchymal stem cells (mMSCs) with oligo-arginine-PEG coated $NaYF_4$:Yb,Er nanoparticles (30 nm) to track the behavior of these cells *in vivo*. Systematic *in vitro* tests revealed that the proliferation and differentiation of mMSCs were not notably affected by UCNP-labeling, suggesting that the cells labeled with oligo-arginine-PEG-UCNPs were able to maintain their stem cell potency. Similarly, Han *et al.*[53] also reported that mesenchymal stem cells labeled with PEI covalently conjugated α-$NaYbF_4$:Tm@CaF_2 were able to undergo osteogenic and adipogenic differentiation upon *in vitro* induction. However, the osteogenesis of labeled rat mesenchymal stem cells appeared to be less potent than that of the unlabeled MSCs. However, we found that specific incubation concentrations such as 400 μg mL^{-1} of citrate-modified $NaLuF_4$:Yb,Tm nanoparitcles (~20 nm) induced a slight influence on the viability of JEG-3 cells, and obvious inhibition of the metastatic ability of JEG-3 cells. As the proliferation and metastatic ability of tumor cells can be regulated by different signaling pathways,[51] this means that inhibition of metastatic ability need not be associated with inhibition of cellular proliferation.

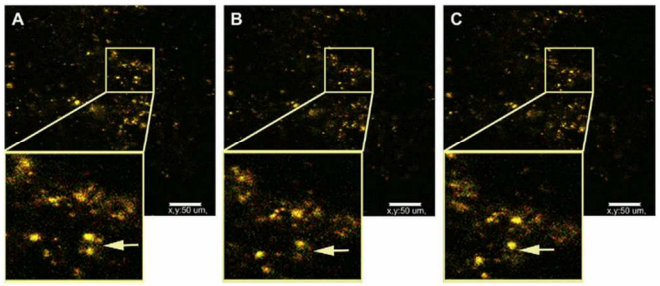

Figure 10. *In vivo* migration of live myoblast cells at (A) 0 h, (B) 2 h and (C) 4 h after treatment of cells with SiO_2-coated $NaYF_4$:Yb,Er nanoparticles (UCNP@SiO_2, 50 nm). scale bar: 50 mm. Reproduced with permission from ref. 52.

6.3 UCNP induced autophagy

Autophagy plays a vital physiological and pathological role in all mammalian cells.[103-106] An elevated level of autophagy, or induced autophagy, is frequently observed in cells under stress conditions. Wen *et al.*[107] showed that after 24 h incubation, HeLa cells stably expressing GFP–LC3 (a fusion protein between Green Fluorescent Protein (GFP) and Microtubule-associated Light Chain 3 (LC3) protein) with 100 μg mL^{-1} uncoated $NaYF_4$:Yb,Er nanoparticles (+22.6 mV, 92 nm), the treated cells showed obvious GFP–LC3 dot formation, indicating autophagy in cells (Figure 11). Moreover, autophagy was also observed in cells incubated with other lanthanide nanoparticles such as Y_2O_3, CeO_2, Yb_2O_3, and Nd_2O_3. However, these results showed that the induced autophagy was dependent on concentration and particle size.

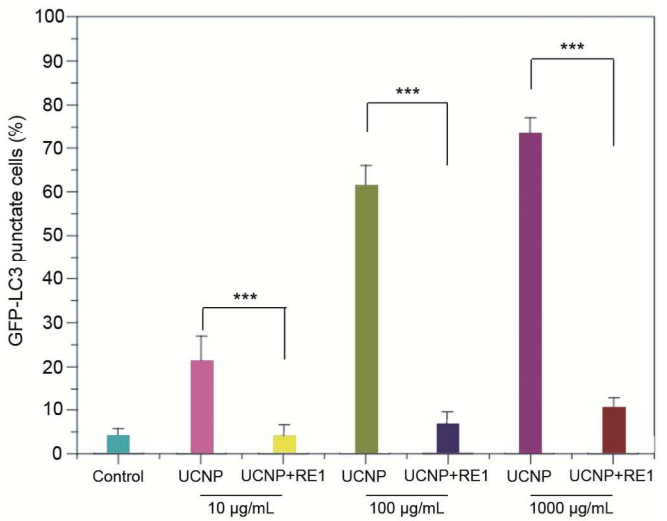

Figure 11. Quantified results of GFP–LC3 punctate HeLa cells treated with the increasing concentrations of uncoated and RE-1-coated UCNP($NaYF_4$:Yb,Er, +22.6 mV, 92 nm, 100 μg mL^{-1}) for 24 h. The lower panels show the. Mean ± s.e.m., n = 3,***P < 0.005. Reproduced with permission from ref. 107.

7. Toxic effects of UCNP *in vivo*

Because lanthanide elements are not known to naturally form part of any biological molecules, the *in vivo* toxicity of UCNPs is one of the most important characteristics regarding the theranostic applications of UCNPs. To date, the *in vivo* toxicity of hydrophilic UCNPs has been systematically investigated in mice, *C. elegans* worms and zebrafish embryos.

7.1 Toxicity of intravenously injected UCNP

Almost all intravenously injected UCNPs are captured by the MPS in organs, such as liver, spleen, lung, and kidney. The long exposure time of UCNPs within living animals gives rise to the possibility of toxicity *in vivo*.

Most of individual studies until now indicated the lanthanide based UCNP was safe at the dosage used for imaging. Zhang *et al.* [67] reported that mice treated with a dose of 10 mg/kg body wt of SiO_2-coated $NaYF_4$:Yb,Er nanoparticles (~30 nm) showed no significant difference in body weight compared to the control group. The observed health status and behavior of all the animals were normal throughout the study. Moreover, all organs weights were consistent among all the animals and at all three experimental times (10 min, 30 min, 24 h and 7 days).

In 2010, we[78] systematically investigated the long-term toxicity of PAA-coated $NaYF_4$:Yb,Er nanoparticles (PAA-UCNPs, 11.5 nm, 15 mg/kg) intravenously injected into mice by observing behaviour, body weight, histology and hematology, and serum biochemistry. No abnormal indicators were observed 115 days after injection, except a small weight difference compared with the control group. Our group observed small weight differences between the mice injected with and without 15 mg/kg wt PAA-UCNPs (~11.5 nm) within 115 days. Compared to the control group, the mice treated with PAA-UCNPs had normal eating

and drinking behavior, fur color, exploratory behavior, activity and neurological status. PAA-UCNPs at a dose of 15 mg/kg wt did not induce abnormal histology in organs such as heart, lung, liver, spleen, and kidney. Cardiac muscle tissue in the heart samples did not show hydropic degeneration. Hepatocytes in the liver samples appeared normal, and there were no inflammatory infiltrates. No pulmonary fibrosis was observed in the lung samples. The glomerulus structure was clear and no necrosis was found in any of the groups. However, the spleen was affected by treatment with PAA-UCNPs, and slight hyperplasia was found in the periarteriolar lymphoid sheath (PALS) of the white pulp. In hematological and serological studies (Figure 12), the blood smears from PAA-UCNPs treated mice indicated that the number and shape of red blood cells, platelets and white blood cells were normal. Alanine aminotransferase, aspartate aminotransferase and total bilirubin were also similar between the mice treated and untreated with PAA-UCNPs. In addition, the toxicity of three UCNP, including $NaGdF_4$:Yb,Er,Tm(26-60 nm, 1.5 mg/kg, 30 day monitoring)[92], DTPA-$NaLuF_4$:Gd,Yb,Er/Tm (80~100 nm, 300 μg/mouse, 30 min monitoring)[35], and 6-aminohexanoic acid modified $NaLuF_4$:Sm,Yb,Tm (~30 nm, 20 mg/kg wt, 7 days monitoring)[108] have been investigated by our group and scarce toxic effects were observed.

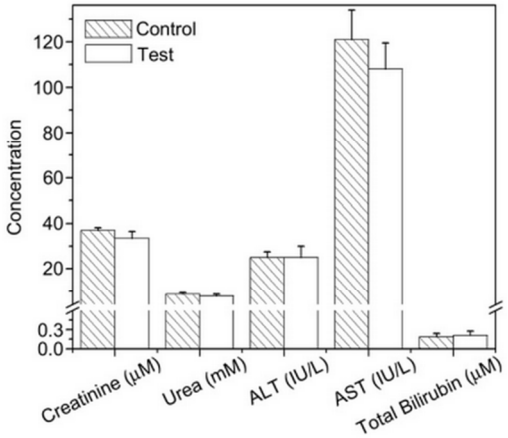

Figure 12. Serum biochemistry indicators of mice injected with PAA-coated $NaYF_4$:Yb,Er nanoparticles (PAA-UCNPs, 11.5 nm, 15 mg/kg) and that receiving no injection(n = 3, Control). Reproduced with permission from ref. 78.

Similarly, Liu *et al.*[83] found no obvious hepatic toxicity induced by intravenous injection of PAA-UCNPs (~35 nm) and PEG-UCNPs (~30 nm), by measuring the levels of aspartate aminotransferase, aspartate aminotransferase, alkaline phosphatase, albumin, globulin and total protein. All of these hematology indicators in the UCNP-treated mouse group appeared normal at several time points post-injection. Blood urea levels in treated mice were also normal. In addition, Recent studies on the mice injected intravenously with some UCNPs for a period of 7~40 days remained healthy and behaved normally. Such UCNPs includes peptide-modifed $NaYF_4$:Yb,Er/Ce nanorods (average diameter: ~55 nm, length: ~25 nm, 200 μg/mouse, 7 days),[109] $BaGdF_5$:Yb/Tm (~10 nm, 10 mg/kg, 40 days),[110] $NaGdF_4$:Yb,Er@$NaGdF_4$@SiO_2 (~150 nm, 1 pM, 30 days),[111] hyaluronic-acid (HA) modified $NaYF_4$:Yb,Gd,Tm (~25 nm, 7 days)[112] and ANG/PEG-UCNPs (~19.3 nm, 15 mg Y/kg)[38]. For example, Yan *et al.*[112] found that, 7 days after injection of HA-modified $NaYF_4$:Yb,Gd,Tm (~25 nm, -27.4 mV) at a dosage of 0.5 mg/mouse for nude mouse and 2.5 mg/mouse for KuMing mouse), showed no significant difference on the body weight and histological analysis was observed between experimental and control group. Shi *et al.*[38] investigated the brain toxicity of ANG/PEG-UCNPs through intravenous route. Compared with the control group, histological analysis of the Kunming mice showed that there were no obvious tissue damage or any other side effect to cortex, hippocampus and striatum of mouse brain.

It should be noted that there are no reports of abnormal behavior and death after intravenous injection of UCNPs in mice even 3 months after injection at the high dose of 15 mg/kg wt.[78]

Although these above-mentioned results indicated the biocompatibility of lanthanide UCNP, more evidence are needed to draw the conclusion that the UCNP are safe. In our recent study, an overdose of intravenously injected citrate modified $NaLuF_4$:Yb,Tm nanophosphors (17 nm) induced obvious toxic effects which were not observed in the low dose group (such as 4 mg/kg wt). Interestingly, the toxic effects were eliminated and organ function recovered 90 days after injection, without any active therapy.[113]

Wen *et al.*[107] found that 24 h after intravenous injection of UCNPs ($NaYF_4$:Yb,Er, +22.6 mV, 92 nm) at a dose of 15 mg kg^{-1} body weight, many autophagosomes were found in liver cells (Figure 13), indicating obvious autophagy. In our recent studies, an overdose of UCNPs by the intravenous route induced obvious toxic effects which were not observed in low dose group (such as 4 mg/kg wt). Interestingly, the toxic effects were eliminated and organ function recovered 90 days after injection without any active therapy.[113]

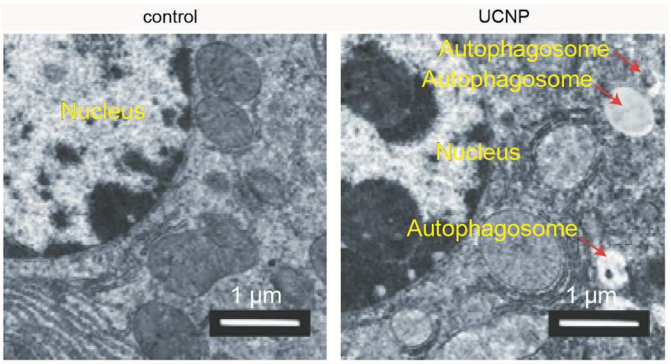

Figure 13. TEM for the liver tissues of mice, 24 h after tail-vein injection with saline (control) or 300 μg of UCNP ($NaYF_4$:Yb,Er, +22.6 mV, 92 nm). Reproduced with permission from ref. 107.

7.2 Toxicity of UCNP to Caenorhabditis elegans and zebrafish models

C. elegans is a free-living nematode with benefits for biosafety assessment, such as relatively short lifecycle, invariable number of cells with complex tissues, complete sequenced genome and so on. There have been several reports on the use of *C. elegans* to investigate UCNPs.[18, 57, 58] For example, after being seeded with PEI-modified $NaYF_4$:Yb,Tm nanoparticles (PEI-UCNPs, 42 nm, 100 μg), these PEI-UCNPs are not excluded by the *C. elegans* during the feeding process, and can be excreted by the body. Moreover, the *C. elegans* incubated with $NaYF_4$:Yb,Tm nanocrystals have normal ingestion behavior as the intact ones. And the protein expression, life span, egg production, egg viability, and growth rate of *C. elegans* fed with the mixture of B-growth media and $NaYF_4$:Yb,Tm nanocrystals have almost the same pattern and ratio of that control.

No significant difference in the ingestion of PEI-UNCPs was observed between the hermaphrodite and the male. Life span, egg production, egg viability, and growth rate showed no obvious differences between the treated and untreated worms.

Toxicity assessments of UNCPs have also been carried out in zebrafish, because zebrafish has small size, rapid development, and short life cycle.[56, 59] Using cardiac myosin light chain 2 transgenic zebrafish modified to express GFP in the heart (Tg(cmlc2:EGFP)) as an animal model, Lee *et al.*[56] investigated the toxic effect of β-$NaYF_4$:Ce,Tb nanoparticles (16.7±0.9 nm) compared to quantum dots (QDs) (Figure 14). The morphology of the heart in the group treated with 500 pM of nanophosphors was similar to that in the control group. The heart in the 500 pM QDs-treated group was significantly smaller and showed the absence of looping in the embryos, indicating delayed development of the heart. The toxicity of lanthanide nanophosphors was only seen at much higher concentrations, and 10 times the number of lanthanide nanophosphors compared with QDs were required to elicit a similar response.

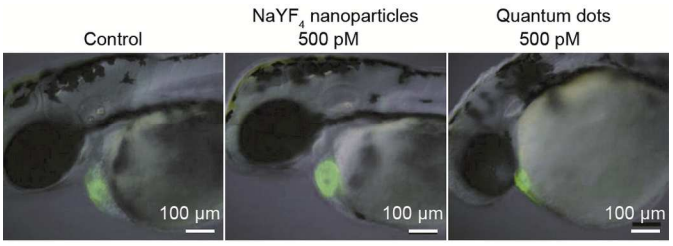

Figure 14. Observation of heart function via Tg(cmlc2:EGFP) zebrafish upon treatment with quantum dots and $NaYF_4$ nanoparticles. Minimal differences in the size and shape of the heart are observed between the control and transgenic zebrafish treated with $NaYF_4$ nanoparticles. On the other hand, those treated with quantum dots show a significantly smaller heart and abnormal morphology.[56] Reproduced with permission from ref. 56.

Recently, Cui *et al.*[74] demonstrated toxic effects of the upconversion LaF_3:Yb,Er@SiO_2 nanophosphors (~10 nm) on zebrafish development after microinjection. They found little effect on the voluntary movements of the tail swing at 24 h post fertilization for the microinjected UCNPs in the range of 5~400 μg mL^{-1}. Moreover, hatching time and hatching success rate of zebrafish decreased with increasing of treatment dose of 5 to 400 μg mL^{-1}. The injection of UCNPs slightly shortened the larval body length and induced malformations. Furthermore, almost all of the individuals treated with the high concentration of UCNPs (200-400 μg mL^{-1}) had severe morphological anomalies with embryonic development. Developmental abnormalities include non-depleted or malformed yolk, spinal, tail and caudal fin malformations, pericardial sac or yolk formations, delayed hatching, stunted body or eye growth, and edema of the body cavity, pericardial sac, or yolk sac regions (Figure 15). Especially, there were increased edema and weak heartbeats in the 200-400 μg mL^{-1} exposed groups compared within the lower dose groups. In addition, the sepn1 gene expression in the exposure groups decreased obviously. One of the reasons of the obvious toxicity may be direct microinjection of such a high dose (400 μg mL^{-1}, 10 nL) of UCNPs into a cell (egg). However, such observation of high UCNPs dose-induced toxicity suggested that the biosafety of lanthanide based UCNP should be paid more attentions.

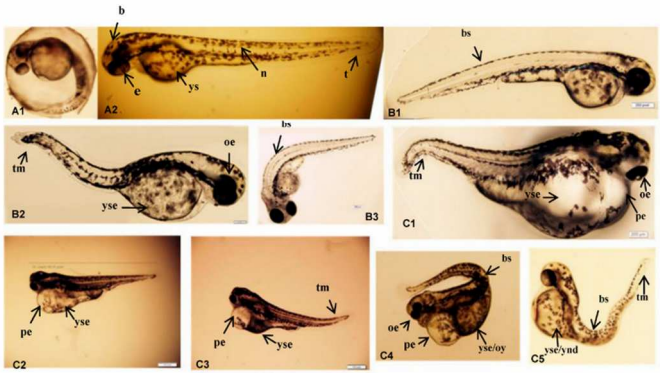

Figure 15. Phenotypic changes of zebrafish embryos at 48 h post fertilization. (A-1, A-2) Control group. (B1-3) UCNPs<200 μg mL^{-1} groups. (C1-5) UCNPs 200-400 μg mL^{-1} groups. Abbreviations: b, brain; e, eye; n, notochord; t, tail; ys, yolk sac; bs, bent spine; tm, tail malformation; oe, ocular edema; pe, pericardial edema; oy, opaque yolk; yes, yolk sac edema; and ynd, yolk not depleted. Reproduced with permission from ref. 74.

7.3 Biosafety assessment of UCNPs on plant

Lanthanide-containing materials generally exist in the environment and are used in agriculture and livestock rearing as fertilizer and feed additives, which are finally deposited in animals or humans. However, little attention has been focused on the interaction between lanthanide nanoparticles and plants.

Recently, our group[114] investigated the effect of citrate-modified $NaLuF_4$:Yb,Tm nanoparticles (cit-UCNPs, ~15 nm) on the germination and growth of mung bean sprouts (Figure 16). Incubation at the high cit-UCNPs concentration of 100 μg mL^{-1} led to growth inhibition of mung beans, and the low concentration of 10 μg mL^{-1} promoted growth. Using confocal microscopy, UCL signals were found in longitudinally cut root, stem, leaf, and seed. After labeling with the radioactive tracer ^{153}Sm, the distribution of ^{153}Sm-labeled cit-UCNPs (cit-UCNPs:^{153}Sm) in the plant (root > seed > leaf > stem) on the

5th day was quantitatively measured by a Geiger counter. Furthermore, when these cit-UCNPs:^{153}Sm-treated bean sprouts were introduced into mouse stomachs, cit-UCNPs:^{153}Sm were excreted with the feces, without adsorption or retention, which was confirmed by SPECT imaging. HE staining showed no detectable toxic effects in the main organs of UCNPs-treated mice. Although the molecular mechanisms of the accelerated growth of bean sprouts are unclear, these studies provide preliminary validation of the biosafety of lanthanide nanophosphors in the environment.

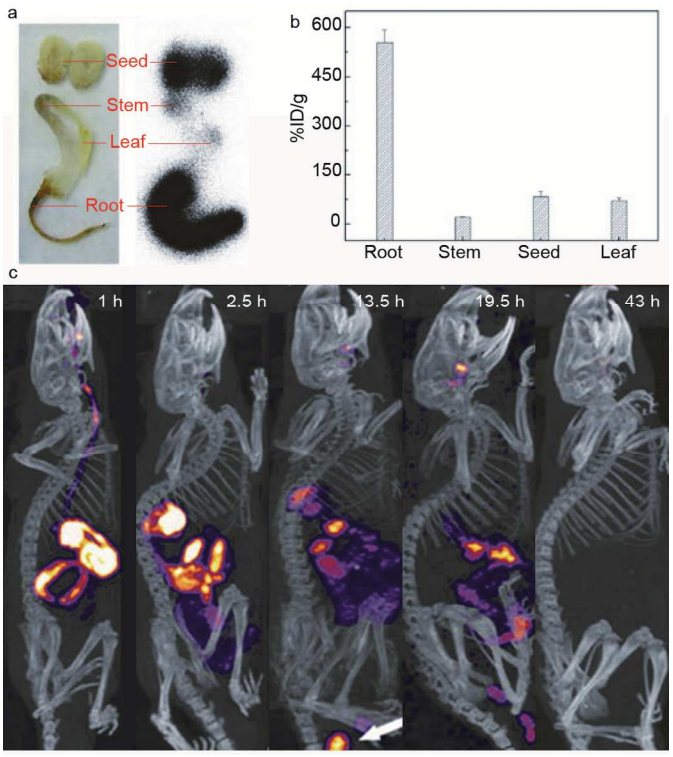

Figure 16. (a) Bright-field image and autoradiography of mung beans treated with ^{153}Sm-cit-UCNPs for 5 days. (b) Radio-distribution of root, stem, seed and leaf of bean sprout treated with ^{153}Sm-cit-UCNPs for 5 days. These data were obtained by distribution experiments and provided as mean±SD of thirteen bean sprouts. (c) Distribution and excretion of orally taken UCNP. Reproduced with permission from ref. 114.

Conclusions and Prospects

This review has covered recent developments concerning the biosafety of lanthanide upconversion nanophosphors. Significant advances have been made in their cellular uptake and cytotoxicity, biodistribution and excretion within living animals.

(1) Tools for studying the safety of UCNPs have developed rapidly. Lanthanide nanoparticles provide rich optical, magnetic, radioactive, and X-ray attenuation properties, by tuning the different 4f electronic structure of the lanthanide elements,[9] and to date, UCL imaging, magnetic resonance imaging (MRI), X-ray computed tomography (CT), SPECT and positron emission tomography (PET) imaging, and ICP-AES techniques have been developed for safety investigations on UCNPs to understand the accurate location and quantity of UCNPs. In particular, the introduction of radioactive imaging techniques such as PET and SPECT, and investigations into the biodistribution of UCNPs will be further accelerated as these will provide rapid quantitative information in living animals.

(2) Almost all of the tested cells, both tumor and normal cells, can internalize UCNPs with an appropriate surface ligand. Most nanoparticles are internalized through endocytosis and remain trapped in endolysosomal vesicles unless co-internalized with a membrane-disrupting agent. The surface-chemical properties of UCNPs play a crucial role in their interaction with cells. Generally, positively charged nanoparticles can effectively cross cell-membrane barriers and localize in the cytosol. Particles of different sizes have different routes of entering cells, and thus it is natural to be concerned regarding the influence of particle aggregation. Under cell incubation conditions, nanoparticles can aggregate to different sizes, which may influence the results and efficiency of the nanomaterial.

(3) Almost all studies show limited effects of the deposition of UCNPs in the MPS. Interestingly, the ratio of UCNPs accumulation in different organs may be significantly altered by surface chemistry techniques, such as PEGlyation, the introduction of targeted moieties, or changing the surface charge. Several strategies have been developed to extend the time in circulation and to enhance the uptake of UCNPs in tumors. Moreover, the behavior of UCNPs administered by different injection routes was observed to be significantly different.

(4) To date, in almost all studies, the elimination of UCNPs was weeks to months, which caused increased exposure time in organs such as the liver, lung and kidney which play critical roles in the human body. Generally, ultrasmall size is essential, but not sufficient for renal excretion. However, UCNPs with ultrasmall size (such as less than 5 nm) show a weak UCL signal due to lattice imperfections, and thus it is not wise to reduce the size to achieve fast and complete elimination by the renal route. When UCNPs were used as a multimodal imaging probe such as an MRI and SPECT probe, it is recommended that the nanoparticle size should be decreased to achieve complete elimination and a low toxicity risk. In addition, surface chemistry used to escape capture by the MPS before excretion was also critical for complete renal elimination. For large UCNPs which cannot be excreted by the renal route, elimination was mainly achieved by the biliary route. The elimination of UCNPs by the biliary route is often slow, ranging from days to months. Although no reliable and effective method has been reported, optimization of the surface property for faster elimination of UCNPs by the biliary route seems to be the best method.

(5) The toxicity of UCNPs is very complicated and remains to be clarified. The assessment of cytotoxicity based on mitochondrial metabolic activity has its limitations. One potential drawback of these metabolic assays is that there is no

differentiation between cells that are actively dividing and those that are quiescent. In addition, cells in different phases have a different degree of mitochondrial metabolic activity. Therefore, cytotoxicity based on the assessment of mitochondrial metabolic activity is not very sensitive at highlighting minor changes and further careful investigation using other accurate tools is necessary in biosafety studies.

In vivo investigation of UCNPs toxicity showed no obvious influence on body weight, behavior, and indicators of histology and hematology at the imaging dose. However, an overdose of UCNPs can induce serious toxic effects, indicating that the toxicity of UCNPs is dose-dependent.

(6) The dose used should be decreased as soon as possible, because the toxicity of UCNPs has been confirmed to be concentration-dependent. Therefore, the quantum yield should be further optimized. The main factors that influence upconversion efficiency are non-radiative decay and the small excitation cross-sections of lanthanide ions, and thus the upconversion efficiency can be improved by increasing the size,[115-117] changing the crystal field symmetry[31, 118-135] and laser annealing[136]. Moreover, the lattice structure of the host, the doping concentration, and the surface surroundings also affect the upconversion efficiency of UCNPs.[137] Therefore, the quantum yield in biological environments can be enhanced.

Acknowledgements

The authors thank State Key Basic Research Program of China of China (2012CB932403 and 2013CB733700), National Science Foundation of China (21231004), and Shanghai Sci. Tech. Comm. (12JC1401300 and 13NM1401101) for financial support.

Notes and references

[a] Department of Chemistry & Institutes of Biomedical Sciences & State Key Laboratory of Molecular Engineering of Polymers, Fudan University, Shanghai 200433, P. R. China. E-mail: fyli@fudan.edu.cn (F. Y. Li); Fax: +86 21-55664621; Tel: +86 21-55664185.

1. F. Auzel, *Chem. Rev.*, 2004, 104, 139-173.
2. Q. Liu, W. Feng and F. Li, *Coordin. Chem. Rev.*, 2014, 273-274, 100-110.
3. Q. Liu, T. S. Yang, W. Feng and F. Y. Li, *J. Am. Chem. Soc.*, 2012, 134, 5390-5397.
4. Q. Liu, B. Yin, T. Yang, Y. Yang, Z. Shen, P. Yao and F. Li, *J. Am. Chem. Soc.*, 2013, 135, 5029-5037.
5. X. G. Liu and F. Wang, *Chem. Soc. Rev.*, 2009, 38, 976-989.
6. S. Gai, C. Li, P. Yang and J. Lin, *Chem Rev*, 2014, 114, 2343-2389.
7. H. H. Gorris and O. S. Wolfbeis, *Angew. Chem. Int. Ed.*, 2013, 52, 3584-3600.
8. M. Haase and H. Schäfer, *Angew. Chem. Int. Ed.*, 2011, 50, 5808-5829.
9. J. Zhou, Z. Liu and F. Y. Li, *Chem. Soc. Rev.*, 2012, 41, 1323-1349.
10. Y. Liu, D. Tu, H. Zhu and X. Chen, *Chem. Soc. Rev.*, 2013, 42, 6924-6958.
11. L. D. Sun, Y. F. Wang and C. H. Yan, *Acc. Chem. Res.*, 2014, 47, 1001-1009.
12. G. Chen, H. Qiu, P. N. Prasad and X. Chen, *Chem. Rev.*, 2014, 114, 5161-5214.
13. J. de Wild, J. K. Rath, A. Meijerink, W. G. J. H. M. van Sark and R. E. I. Schropp, *Sol. Energ. Mat. Sol. C.*, 2010, 94, 2395-2398.
14. F. Wang, Y. Han, C. S. Lim, Y. H. Lu, J. Wang, J. Xu, H. Y. Chen, C. Zhang, M. H. Hong and X. G. Liu, *Nature*, 2010, 463, 1061-1065.
15. J. Zhao, D. Jin, E. P. Schartner, Y. Lu, Y. Liu, A. V. Zvyagin, L. Zhang, J. M. Dawes, P. Xi, J. A. Piper, E. M. Goldys and T. M. Monro, *Nat. Nanotechnol.*, 2013, 8, 729-734.
16. Y. M. Yang, Q. Shao, R. R. Deng, C. Wang, X. Teng, K. Cheng, Z. Cheng, L. Huang, Z. Liu, X. G. Liu and B. G. Xing, *Angew. Chem. Int. Ed.*, 2012, 51, 3125-3129.
17. M. Nyk, R. Kumar, T. Y. Ohulchanskyy, E. J. Bergey and P. N. Prasad, *Nano Lett.*, 2008, 8, 3834-3838.
18. J. C. Zhou, Z. L. Yang, W. Dong, R. J. Tang, L. D. Sun and C. H. Yan, *Biomaterials*, 2011, 32, 9059-9067.
19. S. H. Nam, Y. M. Bae, Y. L. Park, J. H. Kim, H. m. Kim, J. S. Choi, K. T. Lee, T. Hyeon and Y. D. Suh, *Angew. Chem. Int. Ed.*, 2011, 50, 6093-6097.
20. L. Q. Xiong, Z. G. Chen, Q. W. Tian, T. Y. Cao, C. J. Xu and F. Y. Li, *Anal. Chem.*, 2009, 81, 8687-8694.
21. Q. Liu, Y. Sun, T. S. Yang, W. Feng, C. G. Li and F. Y. Li, *J. Am. Chem. Soc.*, 2011, 133, 17122-17125.
22. T. S. Yang, Y. Sun, Q. Liu, W. Feng, P. Y. Yang and F. Y. Li, *Biomaterials*, 2012, 33, 3733-3742.
23. G. Chen, J. Shen, T. Y. Ohulchanskyy, N. J. Patel, A. Kutikov, Z. Li, J. Song, R. K. Pandey, H. Ågren, P. N. Prasad and G. Han, *ACS Nano*, 2012, 6, 8280-8287.
24. Q. Liu, J. J. Peng, L. N. Sun and F. Y. Li, *ACS Nano*, 2011, 5, 8040-8048.
25. H. H. Gorris, R. Ali, S. M. Saleh and O. S. Wolfbeis, *Adv. Mater.*, 2011, 23, 1652–1655.
26. N. Bogdan, F. Vetrone, R. Roy and J. A. Capobianco, *J. Mater. Chem.*, 2010, 20, 7543-7550.
27. L. Zhou, Z. Chen, K. Dong, M. Yin, J. Ren and X. Qu, *Adv. Mater.*, 2013, 26, 2424-2430.
28. L.-L. Li, P. Wu, K. Hwang and Y. Lu, *J. Am. Chem. Soc.*, 2013, 135, 2411-2414.
29. C. Liu, Z. Gao, J. Zeng, Y. Hou, F. Fang, Y. Li, R. Qiao, L. Shen, H. Lei, W. Yang and M. Gao, *ACS Nano*, 2013, 7, 7227-7240.
30. L. Q. Xiong, Z. G. Chen, M. X. Yu, F. Y. Li, C. Liu and C. H. Huang, *Biomaterials*, 2009, 30, 5592-5600.
31. Y. Sun, X. Zhu, J. Peng and F. Li, *ACS Nano*, 2013, 7, 11290-11300.
32. T. Y. Cao, Y. Yang, Y. Gao, J. Zhou, Z. Q. Li and F. Y. Li, *Biomaterials*, 2011, 32, 2959-2968.
33. Y. Sun, M. X. Yu, S. Liang, Y. J. Zhang, C. G. Li, T. T. Mou, W. J. Yang, X. Z. Zhang, B. Li, C. H. Huang and F. Y. Li, *Biomaterials*, 2011, 32, 2999-3007.
34. A. Xia, Y. Gao, J. Zhou, C. Y. Li, T. S. Yang, D. M. Wu, L. M. Wu and F. Y. Li, *Biomaterials*, 2011, 32, 7200-7208.
35. J. Zhou, X. J. Zhu, M. Chen, Y. Sun and F. Y. Li, *Biomaterials*, 2012, 33, 6201-6210.
36. Y. Sun, J. Peng, W. Feng and F. Li, *Theranostics*, 2013, 3, 346-353.
37. G. Chen, T. Y. Ohulchanskyy, W. C. Law, H. Agren and P. N. Prasad, *Nanoscale*, 2011, 3, 2003-2008.
38. D. Ni, J. Zhang, W. Bu, H. Xing, F. Han, Q. Xiao, Z. Yao, F. Chen, Q. He, J. Liu, S. Zhang, W. Fan, L. Zhou, W. Peng and J. Shi, *ACS Nano*, 2014, 8, 1231-1242.
39. Y. I. Park, J. H. Kim, K. T. Lee, K. S. Jeon, H. Bin Na, J. H. Yu, H. M. Kim, N. Lee, S. H. Choi, S. I. Baik, H. Kim, S. P. Park, B. J. Park, Y. W. Kim, S. H. Lee, S. Y. Yoon, I. C. Song, W. K. Moon, Y. D. Suh and T. Hyeon, *Adv. Mater.*, 2009, 21, 4467-4471.
40. D. K. Chatterjee, L. S. Fong and Y. Zhang, *Adv. Drug Deliv. Rev.*, 2008, 60, 1627-1637.
41. Z. Y. Hou, C. X. Li, P. A. Ma, G. G. Li, Z. Y. Cheng, C. Peng, D. M. Yang, P. P. Yang and J. Lin, *Adv. Funct. Mater.*, 2011, 21, 2356-2365.

42. P. Zhang, W. Steelant, M. Kumar and M. Scholfield, *J. Am. Chem. Soc.*, 2007, 129, 4526-4527.
43. S. J. Budijono, J. N. Shan, N. Yao, Y. Miura, T. Hoye, R. H. Austin, Y. G. Ju and R. K. Prud'homme, *Chem. Mater.*, 2010, 22, 311-318.
44. H. Guo, H. Qian, N. M. Idris and Y. Zhang, *Nanomedicine (Lond)*, 2010, 6, 486-495.
45. C. Wang, H. Q. Tao, L. Cheng and Z. Liu, *Biomaterials*, 2011, 32, 6145-6154.
46. N. Lewinski, V. Colvin and R. Drezek, *Small*, 2008, 4, 26-49.
47. S. D. Conner and S. L. Schmid, *Nature*, 2003, 422, 37-44.
48. A. Verma and F. Stellacci, *Small*, 2010, 6, 12-21.
49. J. Jin, Y.-J. Gu, C. Man, J. Cheng, Z. Xu, Y. Zhang, H. Wang, V. Lee, S. Cheng and W.-T. Wong, *ACS Nano*, 2011, 5, 7838-7847.
50. J. Zhou, M. X. Yu, Y. Sun, X. Z. Zhang, X. J. Zhu, Z. H. Wu, D. M. Wu and F. Y. Li, *Biomaterials*, 2011, 32, 1148-1156.
51. A. Asati, S. Santra, C. Kaittanis and J. M. Perez, *ACS Nano*, 2010, 4, 5321-5331.
52. N. M. Idris, Z. Q. Li, L. Ye, E. K. W. Sim, R. Mahendran, P. C. L. Ho and Y. Zhang, *Biomaterials*, 2009, 30, 5104-5113.
53. L. Zhao, A. Kutikov, J. Shen, C. Duan, J. Song and G. Han, *Theranostics*, 2013, 3, 249-257.
54. L. He, L. Feng, L. Cheng, Y. Liu, Z. Li, R. Peng, Y. Li, L. Guo and Z. Liu, *ACS Appl. Mater. Inter.*, 2013, 5, 10381-10388.
55. Y. Bae, Y. Park, S. Nam, J. Kim, K. Lee, H. Kim, B. Yoo, J. Choi, K. Lee, T. Hyeon and Y. Suh, *Biomaterials*, 2012, 33, 9080-9086.
56. G. Jang, M. Hwang, S. Kim, H. Jang and K. Lee, *Biomaterials*, 2014, 35, 440-449.
57. J. Chen, C. Guo, M. Wang, L. Huang, L. Wang, C. Mi, J. Li, X. Fang, C. Mao and S. Xu, *J. Mater. Chem.*, 2011, 21, 2632-2638.
58. S. F. Lim, R. Riehn, W. S. Ryu, N. Khanarian, C. K. Tung, D. Tank and R. H. Austin, *Nano Lett.*, 2006, 6, 169-174.
59. K. Wang, J. Ma, M. He, G. Gao, H. Xu, J. Sang, Y. Wang, B. Zhao and D. Cui, *Theranostics*, 2013, 3, 258-266.
60. S. M. Moghimi, A. C. Hunter and J. C. Murray, *Pharmacol. Rev.*, 2001, 53, 283-318.
61. K. Knop, R. Hoogenboom, D. Fischer and U. S. Schubert, *Angew Chem Int Ed*, 2010, 49, 6288-6308.
62. S. A. Hilderbrand, F. Shao, C. Salthouse, U. Mahmood and R. Weissleder, *Chem Commun*, 2009, 28, 4188-4190.
63. S. J. Budijono, J. Shan, N. Yao, Y. Miura, T. Hoye, R. H. Austin, Y. Ju and R. K. Prud'homme, *Chem. Mater.*, 2009, 22, 311-318.
64. M. Kamimura, D. Miyamoto, Y. Saito, K. Soga and Y. Nagasaki, *Langmuir*, 2008, 24, 8864-8870.
65. T. Cao, Y. Yang, Y. Sun, Y. Wu, Y. Gao, W. Feng and F. Li, *Biomaterials*, 2013, 34, 7127-7134.
66. J. J. Peng, Y. Sun, L. Z. Zhao, Y. Q. Wu, W. Feng, Y. H. Gao and F. Y. Li, *Biomaterials*, 2013, 34, 9535-9544.
67. R. A. Jalil and Y. Zhang, *Biomaterials*, 2008, 29, 4122-4128.
68. X. F. Yu, Z. B. Sun, M. Li, Y. Xiang, Q. Q. Wang, F. F. Tang, Y. L. Wu, Z. J. Cao and W. X. Li, *Biomaterials*, 2010, 31, 8724-8731.
69. N. Bogdan, E. M. Rodriguez, F. Sanz-Rodriguez, M. C. de la Cruz, A. Juarranz, D. Jaque, J. G. Sole and J. A. Capobianco, *Nanoscale*, 2012, 4, 3647-3650.
70. M. Wang, C. C. Mi, W. X. Wang, C. H. Liu, Y. F. Wu, Z. R. Xu, C. B. Mao and S. K. Xu, *ACS Nano*, 2009, 3, 1580-1586.
71. R. Kumar, M. Nyk, T. Y. Ohulchanskyy, C. A. Flask and P. N. Prasad, *Adv. Funct. Mater.*, 2009, 19, 853-859.
72. M. Wang, C. Mi, Y. Zhang, J. Liu, F. Li, C. Mao and S. Xu, *J. Phys. Chem. C*, 2009, 113, 19021-19027.
73. Y. Sun, Q. Liu, J. J. Peng, W. Feng, Y. J. Zhang, P. Y. Yang and F. Y. Li, *Biomaterials*, 2013, 34, 2289-2295.
74. X. Zhu, B. Da Silva, X. Zou, B. Shen, Y. Sun, W. Feng and F. Li, *RSC Adv.*, 2014, 4, 23580.
75. H. S. Choi, W. Liu, P. Misra, E. Tanaka, J. P. Zimmer, B. Itty Ipe, M. G. Bawendi and J. V. Frangioni, *Nat. Biotechnol.*, 2007, 25, 1165-1170.
76. M. Longmire, P. Choyke and H. Kobayashi, *Nanomedicine (Lond)*, 2008, 3, 703-717.
77. G. Ghibellini, E. M. Leslie and K. L. Brouwer, *Mol Pharm*, 2006, 3, 198-211.
78. L. Q. Xiong, T. S. Yang, Y. Yang, C. J. Xu and F. Y. Li, *Biomaterials*, 2010, 31, 7078-7085.
79. H. Xing, W. Bu, Q. Ren, X. Zheng, M. Li, S. Zhang, H. Qu, Z. Wang, Y. Hua, K. Zhao, L. Zhou, W. Peng and J. Shi, *Biomaterials*, 2012, 33, 5384-5393.
80. W. M. Deen, M. J. Lazzara and B. D. Myers, *Am. J. Physiol. Renal. Physiol.*, 2001, 281, F579-596.
81. M. Ohlson, J. Sorensson and B. Haraldsson, *Am. J. Physiol. Renal. Physiol.*, 2001, 280, F396-405.
82. J. L. Bridot, A. C. Faure, S. Laurent, C. Riviere, C. Billotey, B. Hiba, M. Janier, V. Josserand, J. L. Coll, L. V. Elst, R. Muller, S. Roux, P. Perriat and O. Tillement, *J. Am. Chem. Soc.*, 2007, 129, 5076-5084.
83. L. Cheng, K. Yang, M. Shao, X. Lu and Z. Liu, *Nanomedicine (Lond)*, 2011, 6, 1327-1340.
84. R. Naccache, P. Chevallier, J. Lagueux, Y. Gossuin, S. Laurent, L. Vander Elst, C. Chilian, J. Capobianco and M.-A. Fortin, *Adv. Healthc. Mater.*, 2013, 2, 1478-1488.
85. D. K. Chatteriee, A. J. Rufalhah and Y. Zhang, *Biomaterials*, 2008, 29, 937-943.
86. H. Hu, M. X. Yu, F. Y. Li, Z. G. Chen, X. Gao, L. Q. Xiong and C. H. Huang, *Chem. Mater.*, 2008, 20, 7003-7009.
87. Z. L. Wang, J. Hao, H. L. Chan, G. L. Law, W. T. Wong, K. L. Wong, M. B. Murphy, T. Su, Z. H. Zhang and S. Q. Zeng, *Nanoscale*, 2011, 3, 2175-2181.
88. H. Hu, L. Q. Xiong, J. Zhou, F. Y. Li, T. Y. Cao and C. H. Huang, *Chem. Eur. J.*, 2009, 15, 3577-3584.
89. Q. A. Liu, C. Y. Li, T. S. Yang, T. Yi and F. Y. Li, *Chem. Commun.*, 2010, 46, 5551-5553.
90. J. Zhou, L. M. Yao, C. Y. Li and F. Y. Li, *J. Mater. Chem.*, 2010, 20, 8078-8085.
91. Q. Liu, Y. Sun, C. G. Li, J. Zhou, C. Y. Li, T. S. Yang, X. Z. Zhang, T. Yi, D. M. Wu and F. Y. Li, *ACS Nano*, 2011, 5, 3146-3157.
92. J. Zhou, Y. Sun, X. X. Du, L. Q. Xiong, H. Hu and F. Y. Li, *Biomaterials*, 2010, 31, 3287-3295.
93. H. Kobayashi, N. Kosaka, M. Ogawa, N. Y. Morgan, P. D. Smith, C. B. Murray, X. C. Ye, J. Collins, G. A. Kumar, H. Bell and P. L. Choyke, *J. Mater. Chem.*, 2009, 19, 6481-6484.
94. J. N. Shan, S. J. Budijono, G. H. Hu, N. Yao, Y. B. Kang, Y. G. Ju and R. K. Prud'homme, *Adv. Funct. Mater.*, 2011, 21, 2488-2495.
95. J. N. Shan, J. B. Chen, J. Meng, J. Collins, W. Soboyejo, J. S. Friedberg and Y. G. Ju, *J. Appl. Phys.*, 2008, 104, 094308.
96. F. Chen, S. Zhang, W. Bu, X. Liu, Y. Chen, Q. He, M. Zhu, L. Zhang, L. Zhou, W. Peng and J. Shi, *Chem. Eur. J.*, 2010, 16, 11254-11260.
97. M. Deng, Y. Ma, S. Huang, G. Hu and L. Wang, *Nano Res.*, 2011, 4, 685-694.
98. Q. Chen, X. Wang, F. Chen, Q. Zhang, B. Dong, H. Yang, G. Liu and Y. Zhu, *J. Mater. Chem.*, 2011, 21, 7661-7667.
99. S. Jiang and Y. Zhang, *Langmuir*, 2010, 26, 6689-6694.
100. F. Zhang, G. B. Braun, Y. F. Shi, Y. C. Zhang, X. H. Sun, N. O. Reich, D. Y. Zhao and G. Stucky, *J. Am. Chem. Soc.*, 2010, 132, 2850-2851.
101. J. Y. Ryu, H. Y. Park, K. Kim, H. Kim, J. H. Yoo, M. Kang, K. B. Im, R. Grailhe and R. Song, *J. Phys. Chem. C*, 2010, 114, 21077-21082.
102. C. Wang, L. Cheng, H. Xu and Z. Liu, *Biomaterials*, 2012, 33, 4872-4881.
103. N. Mizushima, B. Levine, A. M. Cuervo and D. J. Klionsky, *Nature*, 2008, 451, 1069-1075.
104. B. Levine, *Nature*, 2007, 446, 745-747.
105. T. Pan, S. Kondo, W. Le and J. Jankovic, *Brain*, 2008, 131, 1969-1978.
106. B. Levine, N. Mizushima and H. W. Virgin, *Nature*, 2011, 469, 323-335.

107. Y. Zhang, F. Zheng, T. Yang, W. Zhou, Y. Liu, N. Man, L. Zhang, N. Jin, Q. Dou, Y. Zhang, Z. Li and L.-P. Wen, *Nat. Mater.*, 2012, 11, 817-826.
108. Y. Yang, Y. Sun, T. Y. Cao, J. J. Peng, Y. Liu, Y. Q. Wu, W. Feng, Y. J. Zhang and F. Y. Li, *Biomaterials*, 2013, 34, 774-783.
109. X.-F. Yu, Z. Sun, M. Li, Y. Xiang, Q.-Q. Q. Wang, F. Tang, Y. Wu, Z. Cao and W. Li, *Biomaterials*, 2010, 31, 8724-8731.
110. D. Yang, Y. Dai, J. Liu, Y. Zhou, Y. Chen, C. Li, P. Ma and J. Lin, *Biomaterials*, 2014, 35, 2011-2023.
111. F. Liu, X. He, L. Liu, H. You, H. Zhang and Z. Wang, *Biomaterials*, 2013, 34, 5218-5225.
112. X. Wang, J. T. Chen, H. Zhu, X. Chen and X. P. Yan, *Anal. Chem.*, 2013, 85, 10225-10231.
113. Y. Sun, Doctoral thesis, Fudan University, 2012.
114. J. Peng, Y. Sun, Q. Liu, Y. Yang, J. Zhou, W. Feng, X. Zhang and F. Li, *Nano Res.*, 2012, 5, 770-782.
115. F. Wang, J. Wang and X. Liu, *Angew. Chem. Int. Ed.*, 2010, 49, 7456-7460.
116. J. C. Boyer and F. C. van Veggel, *Nanoscale*, 2010, 2, 1417-1419.
117. J. Zhao, Z. Lu, Y. Yin, C. McRae, J. A. Piper, J. M. Dawes, D. Jin and E. M. Goldys, *Nanoscale*, 2013, 5, 944-952.
118. Q. Cheng, J. H. Sui and W. Cai, *Nanoscale*, 2012.
119. Y. Bai, Y. Wang, K. Yang, X. Zhang, G. Peng, Y. Song, Z. Pan and C. H. Wang, *J. Phys. Chem. C*, 2008, 112, 12259-12263.
120. L. Liu, Y. Wang, X. Zhang, K. Yang, Y. Bai, C. Huang and Y. Song, *Opt. Commun.*, 2011, 284, 1876-1879.
121. X. Chen, Z. Liu, Q. Sun, M. Ye and F. Wang, *Opt. Commun.*, 2011, 284, 2046-2049.
122. Q. Sun, X. Chen, Z. Liu, F. Wang, Z. Jiang and C. Wang, *J. Alloys. Compd.*, 2011, 509, 5336-5340.
123. V. Mahalingam, R. Naccache, F. Vetrone and J. A. Capobianco, *Opt. Express*, 2012, 20, 111-119.
124. G. Chen, H. Liu, H. Liang, G. Somesfalean and Z. Zhang, *J. Phys. Chem. C*, 2008, 112, 12030-12036.
125. H. Liang, Y. Zheng, G. Chen, L. Wu, Z. Zhang and W. Cao, *J. Alloys. Compd.*, 2011, 509, 409-413.
126. Z. Li, B. Dong, Y. He and Z. Feng, *J. Lumin.*, 2012, 132, 1646-1648.
127. G. Tian, Z. Gu, L. Zhou, W. Yin, X. Liu, L. Yan, S. Jin, W. Ren, G. Xing and S. Li, *Adv. Mater.*, 2012, 24, 1226-1231.
128. L. Wang, W. Qin, Z. Liu, D. Zhao, G. Qin, W. Di and C. He, *Opt. Express*, 2012, 20, 7602-7607.
129. W. Yin, L. Zhao, L. Zhou, Z. Gu, X. Liu, G. Tian, S. Jin, L. Yan, W. Ren, G. Xing and Y. Zhao, *Chem.-Eur. J.*, 2012, 18, 9239-9245.
130. L. Guo, Y. Wang, Y. Wang, J. Zhang, P. Dong and W. Zeng, *Nanoscale*, 2013, 5, 2491-2504.
131. D. Li, Y. Wang, X. Zhang, H. Dong, L. Liu, G. Shi and Y. Song, *J. Appl. Phys.*, 2012, 112, 094701.
132. X. Wang, S. Zhao, Y. Zhang and G. Sheng, *J. Rare Earth*, 2010, 28, 222-224.
133. E. L. Cates, A. P. Wilkinson and J.-H. Kim, *J. Phys. Chem. C*, 2012, 116, 12772-12778.
134. J. H. Chung, J. H. Ryu, J. W. Eun, J. H. Lee, S. Y. Lee, T. H. Heo and K. B. Shim, *Mater. Chem. Phys.*, 2012, 134, 695-699.
135. L. Jiang, S. Xiao, X. Yang, J. Ding and K. Dong, *Appl. Phys. B*, 2012, 107, 477-481.
136. A. Bednarkiewicz, D. Wawrzynczyk, A. Gagor, L. Kepinski, M. Kurnatowska, L. Krajczyk, M. Nyk, M. Samoc and W. Strek, *Nanotechnology*, 2012, 23, 145705.
137. M. C. Tan, L. Al-Baroudi and R. E. Riman, *ACS Appl Mat Inter*, 2011, 3, 3910-3915.
138. Q. Liu, M. Chen, Y. Sun, G. Y. Chen, T. S. Yang, Y. Gao, X. Z. Zhang and F. Y. Li, *Biomaterials*, 2011, 32, 8243-8253.
139. Z. Liu, Z. Li, J. Liu, S. Gu, Q. Yuan, J. Ren and X. Qu, *Biomaterials*, 2012, 33, 6748-6757.
140. Q. Xiao, W. Bu, Q. Ren, S. Zhang, H. Xing, F. Chen, M. Li, X. Zheng, Y. Hua, L. Zhou, W. Peng, H. Qu, Z. Wang, K. Zhao and J. Shi, *Biomaterials*, 2012, 33, 7530-7539.
141. Y. Wang, L. Ji, B. Zhang, P. Yin, Y. Qiu, D. Song, J. Zhou and Q. Li, *Nanotechnology*, 2013, 24, 175101.
142. L. Cheng, K. Yang, S. Zhang, M. W. Shao, S. T. Lee and Z. Liu, *Nano Res.*, 2010, 3, 722-732.
143. D. Yang, X. Kang, P. Ma, Y. Dai, Z. Hou, Z. Cheng, C. Li and J. Lin, *Biomaterials*, 2013, 34, 1601-1612.
144. W. Zhang, B. Peng, F. Tian, W. Qin and X. Qian, *Anal. Chem.*, 2014, 86, 482-489.
145. J. W. Shen, C. X. Yang, L. X. Dong, H. R. Sun, K. Gao and X. P. Yan, *Anal. Chem.*, 2013, 85, 12166-12172.
146. L. Cheng, K. Yang, M. W. Shao, S. T. Lee and Z. Liu, *J. Phys. Chem. C*, 2011, 115, 2686-2692.
147. H. Li and L. Wang, *Chinese Sci. Bull.*, 2013, 58, 4051-4056.
148. H. Liu, W. Lu, H. Wang, L. Rao, Z. Yi, S. Zeng and J. Hao, *Nanoscale*, 2013, 5, 6023-6029.
149. D. Yang, Y. Dai, P. a. Ma, X. Kang, M. Shang, Z. Cheng, C. Li and J. Lin, *J. Mater. Chem.*, 2012, 22, 20618.
150. G. Gao, C. Zhang, Z. Zhou, X. Zhang, J. Ma, C. Li, W. Jin and D. Cui, *Nanoscale*, 2013, 5, 351-362.
151. Q. Chen, C. Wang, L. Cheng, W. He, Z. Cheng and Z. Liu, *Biomaterials*, 2014, 35, 2915-2923.
152. S. Zeng, M.-K. K. Tsang, C.-F. F. Chan, K.-L. L. Wong, B. Fei and J. Hao, *Nanoscale*, 2012, 4, 5118-5124.
153. S. Zeng, M. K. Tsang, C. F. Chan, K. L. Wong and J. Hao, *Biomaterials*, 2012, 33, 9232-9238.
154. J.-n. Liu, W. Bu, L.-m. Pan, S. Zhang, F. Chen, L. Zhou, K.-l. Zhao, W. Peng and J. Shi, *Biomaterials*, 2012, 33, 7282-7290.
155. L. Dong, D. An, M. Gong, Y. Lu, H. L. Gao, Y. J. Xu and S. H. Yu, *Small*, 2013, 9, 3235-3241.
156. G. Ajithkumar, B. Yoo, D. E. Goral, P. J. Hornsby, A.-L. Lin, U. Ladiwala, V. P. Dravid and D. K. Sardar, *J. Mater. Chem.*, 2013, 1, 1561.
157. H. Xing, W. Bu, S. Zhang, X. Zheng, M. Li, F. Chen, Q. He, L. Zhou, W. Peng, Y. Hua and J. Shi, *Biomaterials*, 2012, 33, 1079-1089.
158. C. Li, Z. Hou, Y. Dai, D. Yang, Z. Cheng, P. a. Ma and J. Lin, *Biomat. Sci.*, 2013, 1, 213.
159. J. Liu, W. Bu, S. Zhang, F. Chen, H. Xing, L. Pan, L. Zhou, W. Peng and J. Shi, *Chem.-Eur. J.*, 2012, 18, 2335-2341.
160. C. Li, D. Yang, P. Ma, Y. Chen, Y. Wu, Z. Hou, Y. Dai, J. Zhao, C. Sui and J. Lin, *Small*, 2013, 9, 4150-4159.
161. P. Ramasamy, P. Chandra, S. W. Rhee and J. Kim, *Nanoscale*, 2013, 5, 8711-8717.
162. Q. Xiao, X. Zheng, W. Bu, W. Ge, S. Zhang, F. Chen, H. Xing, Q. Ren, W. Fan, K. Zhao, Y. Hua and J. Shi, *J. Am. Chem. Soc.*, 2013, 135, 13041-13048.
163. A. Xia, M. Chen, Y. Gao, D. Wu, W. Feng and F. Li, *Biomaterials*, 2012, 33, 5394-5405.
164. X. J. Zhu, J. Zhou, M. Chen, M. Shi, W. Feng and F. Y. Li, *Biomaterials*, 2012, 33, 4618-4627.
165. S. H. Gao, F. Y. Liu, B. T. Zhang, Y. J. Wang, H. M. Zhang and Z. X. Wang, *Chinese J. Anal. Chem.*, 2013, 41, 811-816.
166. S. Jeong, N. Won, J. Lee, J. Bang, J. H. Yoo, S. G. Kim, J. A. Chang, J. Kim and S. Kim, *Chem. Commun.*, 2011, 47, 8022-8024.
167. H. T. Wong, M. K. Tsang, C. F. Chan, K. L. Wong, B. Fei and J. Hao, *Nanoscale*, 2013, 5, 3465.
168. Y. I. Park, H. M. Kim, J. H. Kim, K. C. Moon, B. Yoo, K. T. Lee, N. Lee, Y. Choi, W. Park, D. Ling, K. Na, W. K. Moon, S. H. Choi, H. S. Park, S.-Y. Yoon, Y. D. Suh, S. H. Lee and T. Hyeon, *Adv. Mater.*, 2012, 24, 5755-5761.

Table 1. Biodistribution *in vivo* of lanthanide upconversion nanophosphors.

UCNP	surface	Concentration	Size (nm)	Time (h)	Distribution site and the dosage[a,b]	ref
$NaYF_4$:Yb,Er	SiO_2	10 mg kg^{-1}	21±0.5	0.5	L (18.6 mg/L/g), H (10.9 mg/L/g), S (6.3 mg/L/g), K (3.9 mg/L/g)	67
$NaYF_4$:Yb,Er/Tm	PEI, PEI	4.4 mg mL^{-1}	50	0.5	L (20 mg Y/g), H (～3.0 mg Y/g), S (～2.5 mg Y/g), K (～2.0 mg Y/g)	85
$NaYF_4$:Yb,Er	FA	100 μg/animal	20	24	S (～35 μg of Y/g), L (～9 μg Y/g), lung (～7 μg Y/g), K (～7 μg Y/g), H (～4 μg of Y/g)	30
$NaYF_4$:Yb,Tm	PAA	15 mg kg^{-1}	11.5	24	S (～7 ID/g), L (～0.9 ID/G), L (～0.1 ID/g)	78
$NaYF_4$:Yb,Er/Ce	CTX	1.0 mg mL^{-1}	55	24	L (～85 μg Y/g), S (～82 μg Y/g), L (～20 μg of Y per g), K (～4μg of Y/g), H (～3μg of Y/g)	68
$NaGdF_4$:Yb,Tm,Er	OA	1.0 mg mL^{-1}	25～60	~0.7	S (12.4%), L (7.51%), L (1.21%), M (0.79%), H (0.63%), K (0.57%)	92
$NaYF_4$:Yb,Er/Tm	PAA/PEG	2.0mg mL^{-1}	30	24	S (～240% ID/g), L (～95% ID/g), L (～40% ID/g), B (～20% ID/g)	83
$NaYF_4$:Yb,Tm	OA, CD	0.5 mg mL^{-1}	18	2	S (～118.9% ID/g), L (～57.6% ID/g)	138
$NaYF_4$:Yb,Tm	Citrate	1.25 mg mL^{-1}	20	2	S (～73.0% ID/g), L(～53.0%ID/g)	33
$NaYF_4$:Yb,Er	PEG	20 mg mL^{-1}	30	24	Skin (～140 μg Y/g), S (～50 μg Y/g), muscle (～30μg Y/g), L (～20μg Y/g)	45
$NaYF_4$:Gd,Yb,Er	citrate	0.5mg mL^{-1}	28.2	0.25	L (70.8% ID/g), S (55.7% ID/g)	50
Yb_2O_3:Er	PEG	1.0 mg mL^{-1}	175±32.6	24	L (～48% ID/g), S(～22% ID/g), K (～23%ID/g), L(～5% ID/g)	139
$NaYF_4$:Yb,Er	PEG, poly-Arginine	0.1 mg mL^{-1}	30	1	L (relative UCL intensity: ～20000 a.u.), L (～2000 a.u.), S (～1000 a.u.)	102
$NaYF_4$:Yb,Er,Tm@$NaGdF_4$@TaO_x	PEG	8.0 mg mL^{-1}	30	0.5	L (HU:110.2), S (HU:80.6), H (HU:70.4), K (HU:58.9)	140
$NaYF_4$:Yb,Er	PEG	2.0 mg mL^{-1}	5±2.2	1	L (36.93±5.80%ID/g), S (25.71±9.40%ID/g)	65
pSi@$NaGdF_4$:Yb,Er@$NaGdF_4$	F127	2 pmol	150	~0.17	Bladder (HU: 52), L (50), S (48), K (44.8/45.1), H(41.9)	111
$NaLu(Gd)F_4$:Yb,Tm	Citrate	2 mg mL^{-1}	60	5	L (～130% ID/g), S(～80% ID/g), B (～20% ID/g)	73
$NaYF_4$:Yb,Er,La@DTPA-Gd	PEG	1.0 mg kg^{-1}	32–86	2	L (～14%ID/g), S (～9%ID/g), L (～2.5%ID/g), H (～1.8%ID/g), K (～1.6% ID/g)	141
$NaLuF_4$:Yb,Tm	AA[a]	2.0 mg mL^{-1}	45	1	L (～56% ID/g), S (～20% ID/g)	108

[a] A portion of quantification data of distribution was estimated according to the Figure shown in the articles, because of no accurate dictation in the paper.

[b] H, heart; L, liver; S, spleen; L, lung; K, kidney; B, bone; M, muscle.

Table 2. Cell viability after incubation with UCNPs.

UCNP	Surface	Size (nm)	Incubation time (hours)	Incubation concentration (μg mL^{-1})	Viability %	cell line	Ref
$NaYF_4$:Yb,Er	FA, OA−PAA−PEG, AA, F127, PEG, PEI, Poly-OEGMA[a]	5~130	2; 24	5~1000	>90	HeLa, KB, L929, CL, HCCHM3	30, 33, 65, 142-144
$NaYF_4$:Yb,Tm	FA, PAA	21~39	24; 48	480~600	>94	HeLa, KB	78, 145
$NaYF_4$:Yb,Er,Tm	PEG-$PMHC_{18}$[a], PEG, PEG-RGD[a], OCMC[a]	25.8~335	10; 24; 48; 216	0~1000	>80	U87MG, HeLa	20, 93, 146, 147
$NaY(Gd)F_4$:Yb,Er	Citrate	28.2	24	500	81	KB	50
$NaY(Gd)F_4$:Yb,Tm	ANG[a],PEG	17.2~19.3	24	1000	>85	U87MG, BCECs	38
$NaYF_4$:Yb,Er,La	GdDTPA	32~86	48	400	>85	L929	141
$BaYF_5$:Yb,Er	PEI	24	24	1000	83	HeLa	148
$LiYF_4$:Yb,Er	SDS[a]	17~20	24	200	~100	L929	149
$NaGdF_4$:Yb,Er	F127, PAA, BSA	10.5~100	24	400~500; 60 pM	>85	HeLa, GES-1, SW480, 4T1	111, 150, 151
$BaGdF_5$:Yb,Er	PEI, PEG	10~12	24	500	>80	HeLa	152, 153
$BaGdF_5$:Yb,Tm	gelatin	<10	24	200	~100	L929	110
$NaLuF_4$:Yb,Tm	Citrate, PEG	17~20	24; 48	600~1000	>85	KB	36, 66
$NaLuF_4$:Yb,Er,Tm	GdDTPA	80~100	24	800	~90	HeLa	35
$NaYF_4$:Yb,Er@$NaGdF_4$	ANG, PEG	49.6~62.6	24	1000	~100	HeLa	154
$NaYF_4$:Yb,Er,Tm@$NaGdF_4$	PEG	~30	24	1000	>80	RAW264.7	140
Yb_2O_3:Er	PEG	140~200	48	1000	~100	HepG2	139
Y_2O_3:Yb,Er	PEG	<200	24	1000	96	HeLa	155
Gd_2O_2S:Yb,Er	-	~10	48	200	94.3	SK-N-SH	156
$NaYF_4$:Gd,Yb,Er,Tm@SiO_2	PEG	~25	24	800	~90	MCF-7	157
$NaYF_4$:Yb,Er@mSiO_2	PEG-FA	~80	24	50	~80	L929	158
$NaY(Gd)F_4$:Yb,Tm@mSiO_2	-	34	24	250	>90	MCF-7	159
$NaYF_4$:Yb,Er@mSiO_2	PEG	22	24	400	~100	L929	160
$NaGdF_4$:Yb,Er,Fe@SiO_2	FA	~20	24	1000	>89	HeLa	161
$NaYb(Gd)F_4$:Er@SiO_2/CuS	PEG	45	24	600	87	HeLa	162
$NaLuF_4$:Yb,Tm@SiO_2	DTPA	30~40	24	500	>80	HeLa, LO2	163
$NaYF_4$:Yb,Tm@Fe_xO_y	dopamine	30	48	100	>80	KB	34
$NaLuF_4$:Yb,Er,Tm@Fe_3O_4	-	~330	24	800	85	HeLa	164
$NaYF_4$:Yb,Er@TaOx	-	~35	24	2500	>90	HeLa	165
$NaYF_4$:Yb,Tm	CTAB[a]	~18	24	100	<10	HeLa	166
$NaGdF_4$:Yb,Er	PEG, PEI	~30	24	1000	>50	HeLa	54
$KGdF_4$:Yb,Er	PEI	~14	24	500	>60	HeLa	167
$NaYF_4$:Yb,Er@$NaGdF_4$	PEG	62.6	24	130	~60	U87MG, GES1	168

[a] OEGMA, oligo(ethylene glycol) methacrylate; $PMHC_{18}$, poly(maleic anhydride-alt-1-octadecene); RGD, arginine-glycine-aspartate tripeptide; OCMC, oxidized carboxymethyl cellulose; ANG, Angiopep-2; SDS, sodium dodecylsulfate; BSA, bovine serum albumin; CTAB, cetyltrimethylammonium bromide.

TOC Figure

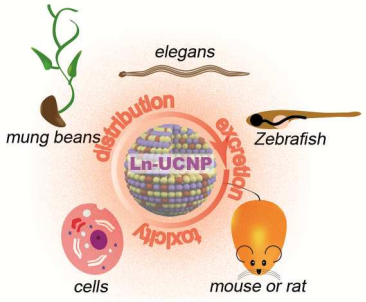

The association between the chemo-physical properties of UCNPs and their biodistribution, excretion, and toxic effects is presented in this review.

Dr. Yun Sun *was born in Shandong, China, in 1982. He received his PhD (2012) from Fudan University under the direction of Prof. Chunhui Huang and Prof. Fuyou Li.. He worked as a postdoctoral researcher at Fudan University from 2012–2014. His research interest focus on the bioapplication and biosafety of multifunctional rare-earth nanomaterials.*

Dr. Wei Feng *received his B. S. degree in 2004 and Ph. D. degree in 2009, both in chemistry from Peking University. He subsequently worked as postdoctor on the synthesis and applications of upconversion nanomaterials with Prof. Chunhua Yan in Peking University for two years. He is currently a lecturer in the Department of Chemistry at Fudan University. His research interests lie in design and synthesis of luminescent nanomaterials with focus on their biological applications.*

Prof. PengyuanYang*, got his Bachelor in Chemistry at Inner-Monguliar University major in Chemistry; Master Degree at Science and Technology University of China, under supervision of Prof. Zheming Ni; Ph D at the University of Massachusetts at Amherst under supervision of Prof. RM Barns, both degrees in Analytical Chemistry. He was Postdoctoral Fellow in Indiana University at Bloomiongton under Prof. GM Hieftje, and in Xiamen University under Prof. Benli Huang. He is currently the Deputy Director of Institutes of BioMedical Sciences, Fudan University, Shanghai China. He pecializes in Mass-Spectrometry based technology and methodology, and is very active in the fields of bio-mass spectrometry, proteomics and bio-application of nano-materials, especially in the field of Biomass Spectrometry and its application in Proteomics and in cancer studies.*

Prof. Chunhui Huang *graduated from Peking University in 1955, since then she worked as an assistant, associate and full professor at Chemistry Department, Peking University from 1955 to present. She became a member of the Chinese Academy of Science in 2001. In 2003 she also established a research group in Fudan University cooperating with professor Fuyou Li and Tao Yi. More than 400 scientific papers and three books have been published under her name. Her current research interests focus on coordination chemistry and functional materials for optics and electronics.*

Fuyou Li *was born in Zhejiang, China, in 1973. He received his PhD (2000) from Beijing Normal University. He worked as a postdoctoral researcher at Peking University from 2000–2002. He worked as an associate professor at Peking University from 2002-2003 and Fudan University from 2003-2006. He has been working as a full Professor at Fudan University since 2006. His current research interests involve multifunctional rare-earth nanomaterials and phosphorescent metal-complexes for bioimaging. To date, his research records 130 scientific publications.*